CO_2 storage – Simulations for forecasting the behavior of injection CO_2 in geological formations

Van Thi Hai Pham

Dissertation for the degree of Philosophiae Doctor (Ph.D.)

Department of Geosciences
Faculty of Mathematics and Natural Sciences
University of Oslo, Norway

Submitted: November 2012

Series of dissertations submitted to the
Faculty of Mathematics and Natural Sciences, University of Oslo
No. 1313

ISSN 1501-7710

Cover: Inger Sandved Anfinsen.
Printed in Norway: AIT Oslo AS.

Produced in co-operation with Akademika publishing.
The thesis is produced by Akademika publishing merely in connection with the thesis defence. Kindly direct all inquiries regarding the thesis to the copyright holder or the unit which grants the doctorate.

Preface

This thesis is entitled 'CO_2 storage – Simulations for Forecasting the Behavior of Injection CO_2 in Geological Formations'. The thesis has been submitted to the Department of Geosciences at University of Oslo in accordance with the requirements for the degree of Philosophiae Doctor (Ph.D) in Environmental-Petroleum Geology. The study herein was completed as part of a larger project entitled "SSC-Ramore: Subsurface storage of carbon dioxide - risk assessment, monitoring and remediation", funded by the Norwegian Research Council under the CLIMIT program, and also supported by Statoil Statoil Hydro, ConocoPhillips, Norske Shell, RWE Dea and Schlumberger. The purpose of the study was to investigate the geochemical interaction of CO_2 with cap-rocks and the behavior of CO_2 injected in storage sites.

The introduction of the thesis consists of a brief description of the scope and objectives, some background information on storage mechanisms for CO_2 and the models we applied for addressing the necessary questions for obtaining our goals. This is followed by a summary of the papers and, finally, some concluding remarks.

The main focus of this study was to simulate and predict the behavior of the CO_2 plume in the reservoir, the geochemical and the ultimate fate of CO_2 in the reservoir formations.

Acknowledgements

First and foremost I would especially like to thank my advisors Professor Per Aagaard, Dr. Helge Hellevang, Professor Bjørn Kvamme and Dr. Ingrid Anne Munz for the opportunity to work with them and for their advice, support and contributions to this work. I would like to thank everyone who has helped me during the period I was learning and studying at the Department of Geosciences, University of Oslo. Thanks to all my colleagues at University of Oslo and Norwegian Petroleum Directorate (NPD) for their help, the discussions on both research subjects and non- academic topic such as during the open lunches.

The SSC-Ramore project is a cooperative effort between University of Oslo, University of Bergen, NGI and IFE, with the support of partners from industry toward solving environmental challenges. I would like to acknowledge the economic support by the Norwegian Research Council and the following companies: Statoil Hydro, ConocoPhillips, Norske Shell, RWE Dea and Schlumberger, as well as the NPD for providing data.

I would also like to acknowledge the following persons: Amy Dale, who helped me to correct the English language in the first academic article and the thesis, and Michael Heeremans who helped me to collect the valuable data needed to build the reservoir models.

Last but not least, I want to thank my parents, my little daughter and my friends for their encouragement during the past few years making it possible for me to finish this study.

Contents

List of Publications

Paper 1: **V.T.H. Pham**, P. Lu, P. Aaagaard, C. Zhu and H. Hellevang. (2011). On the potential of CO_2-water-rock interactions for CO_2 storage using a modified kinetic model. International Journal of Greenhouse Gas Control, 5: 1002 - 1015.

Paper 2: **V.T.H. Pham**, P. Aagaard and H. Hellevang. (2012). On the potential for CO_2 storage in continental flood basalts. Geochemical Transactions, 13:12 pp.

Paper 3: **V.T.H. Pham**, I.T. Gjeldvik, F. Riis, E. K. Halland, I. M. Tappel, P. Aagaard. Assessment of CO_2 injection into the south Utsira-Skade aquifer, the North Sea, Norway. International Journal of Energy (Reviewed January 2013).

Paper 4: H. Hellevang, **V.T.H. Pham** and P. Aagaard. Kinetic modeling of CO_2-water-rock interactions. International Journal of Greenhouse Gas Control (Accepted for publication 2013).

Extended abstract: V.T.H. Pham, Maast T. E, H. Hellevang and P. Aagaard (2011). Numerical modeling including hysteresis properties for CO_2 storage in Tubåen Formation, Snøhvit Field, Barents Sea. Energy Procedia, 4: 3746 - 3753

1. Introduction

1.1 CO_2 injection in the sub-surface

Historical development

CO_2 storage is one of the proposed solutions for mitigating the amount of CO_2 released into the atmosphere and helping to reduce the effect of global warming (Holloway, 2004). CO_2 has been injected into geological formations during commercial operations like the Acid-gas Deep Injection in Canada (Bachu and Gunter, 2004), the Sleipner (Torp and Gale, 2004) and Snøvhit projects in Norway) (Maldal and Tappel, 2004), the In Salah project in Algeria (Riddiford et al., 2003) and is now planned in the Gorgon field in Australia (Flett et al., 2009; Flett et al., 2007). Pilot or demonstration projects have been launched such as the Frio & RCSP-phase II in the USA, Ketzin in Germany, Lacq/Rousse in France and Otway I&II in Australia (Michael et al., 2010).

Figure 1 Map showing active CO_2 storage projects that have injected CO_2 into deep saline aquifers and some planned projects that are planned, including small-scale injections into saline aquifers, depleted gas/oil fields, and enhanced oil/gas recovery (EOR/EGR) projects, as reported by Michael et al. (2010). The Lacq (Rousse) site has been added subsequently.

The first commercial project injecting CO_2 and H_2S into a saline aquifer was the Acid Gas Deep Injection project in Canada in the early 1990s (Bachu and Gunter, 2004). The Sleipner project on the Norwegian continental shelf was started in 1996 and was the first commercial-scale project involving the injection of CO_2 gas only into a saline aquifer (see Figure 1 and Table 1) (Torp and Gale, 2004). Projects involving the injection of CO_2 from natural gas production started in In Salah, Algeria (Riddiford et al., 2003) and Snøhvit, offshore Norway (Maldal and Tappel, 2004) in 2004 and 2008, respectively. Snøhvit, Sleipner and In Salah are the largest commercial injection operations today and they have the highest injection rate to date (Table 1) with a life-time injection that is planned to last more than 10 years. The experience gained from these three operations is very valuable and demonstrates how CO_2 injection and storage occur in different types of reservoirs (Eiken et al., 2011; Hermanrud et al., 2009).

In addition, CO_2 is being injected into depleted oil/gas reservoirs at some localities to increase and enhance oil/gas recovery. Weyburn, Canada, is an enhanced oil recovery (EOR) project (Riding, 2006; Riding et al., 2003), and there are enhanced gas recovery (EGR) projects in Otway, Australia (Bouquet et al., 2009) and K12B in the Netherlands (Van Der Meer et al., 2005) (see Figure 1). In France, Total's Carbon Capture and storage (CCS) pilot project involves two different sites: 1) Lacq, where the CO_2 is captured from the exhaust gases of an existing boiler, and 2) the Rousse gas field, where the CO_2 is injected into a depleted natural gas reservoir.

Table 1 List of operations injecting or having injected CO_2 into saline aquifers, as of Dec. 2009. Some projects in an advanced planning stage are also shown and the list continues to grow (Michael et al., 2010). Lacq (Rousse) has been added subsequently.

Project name	Location	Scale	Status	Inj. start	Inj. finish	Inj. rate (t/day)	Total (kt)
Frio	Liberty County, Texas, USA	Pilot	Completed	Frio 1 2004 Frio 2 2006	Frio 1 2004 Frio 2 2006	250	1.6
Nagaoka	Nagaoka City, Japan	Pilot	Completed	2003	2005	40	10
Ketzin	Ketzin, Brandenburg, Germany	Pilot	Ongoing	2008	2010	86	60
Alberta Basin (Acid Gas)	Alberta & B.C., Canada	Commercial	Ongoing	1990		5–190	
Snøhvit	Barents Sea, Norway	Commercial	Ongoing	2008		2000	23,000
Sleipner	North Sea, Norway	Commercial	Ongoing	1996		2700	20,000
In Salah	Krechba, Algeria	Commercial	Ongoing	2004		3500	17,000
Gorgon	Barrow Island, WA, Australia	Commercial	Approved	2014		12,300	129,000
MGSC Decatur	Decatur, IL, USA	Demonstration	Ongoing	2010	2012	1000	1000
Lacq/Rousse	Lacq, France	Demonstration	Ongoing	2010		205	
MRCSP Appalachian Basin	Shadyside, OH, USA	Pilot	No injectivity	2008	2009	–	–
MRCSP - Cincinnati Arch	Kentucky, USA	Pilot	Monitoring underway	2009	2009	500	1
MRCSP Michigan Basin	Gaylord, MI, USA	Pilot	Monitoring underway	2008	2009	300–600	60
SECARB Mississippi	Escatawpa, MS, USA	Pilot	Completed	2008	2008	160	2.75
SECARB Early	Cranfield, MS, USA	Demonstration	Ongoing	2009	2010	2700	1500
WESTCARB Arizona Utilities	Northeast Arizona, USA	Pilot	No injectivity	2009	2009		

Potential storage sites

For CO_2 injection and storage in subsurface formations, a criterion required for site selection is that CO_2 is in a supercritical state. Supercritical CO_2 has high density and behaves like a fluid. It is lighter than water and therefore has a tendency to migrate upwards in a saline aquifer by the force of buoyancy. Supercritical CO_2 then behaves like hydrocarbons and accumulates in traps under the surface. The experience of the operation in the oil and gas industry could also apply to CO_2 injection and storage. The main difference between CO_2 and hydrocarbons involves their different phase behavior and their solubility in water, factors that could be considered and adjusted.

CO_2 can be stored in the same types of traps as hydrocarbon accumulations (Figure 2). Major categories of structural traps include (A) fold, (B) fault, (C) piercement, (D) combination fold-fault, (E) sub-unconformities and (F) above conformities (Biddle and Wielchowsky, 1994). Primary or depositional stratigraphic traps were categorized as traps created by lateral changes in sedimentary rock type during deposition, with the reservoir and seal being created by lateral facies changes (Figure 2 G1), and reservoir termination due to the depositional pinching out of porous and permeable rock units (Figure 2 G2). Traps formed by buried depositional relief (Figure 2H) (Biddle and Wielchowsky, 1994). In each example, sedimentary processes form a potential trapping geometry, but require burial by a younger impermeable section to create the required top seal.

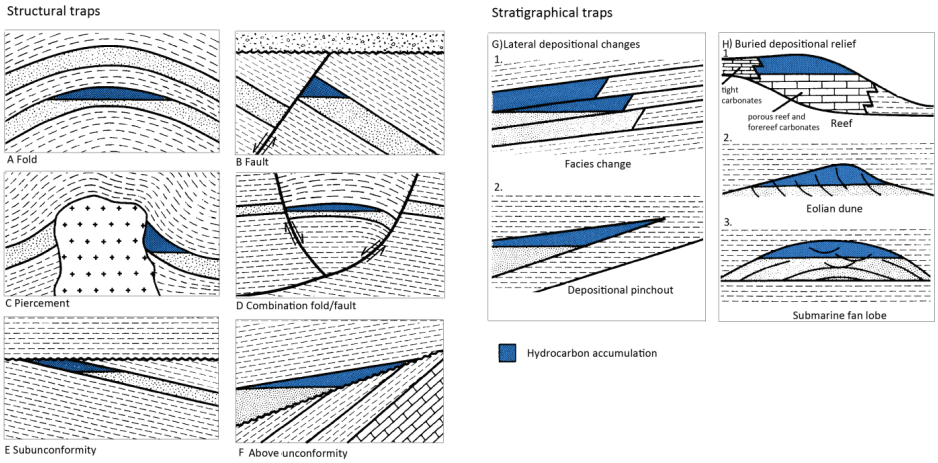

Figure 2 Major categories of structural and stratigraphical traps (Biddle and Wielchowsky, 1994)

If the volume of CO_2 injected is small compared to the storage formation, the CO_2 may be trapped by migrating laterally beneath the seal, as the migration distance does not reach the edge limit of the cap-rock (see Figure 3). In such cases, it is possible to store CO_2 in a large area without a closed structure.

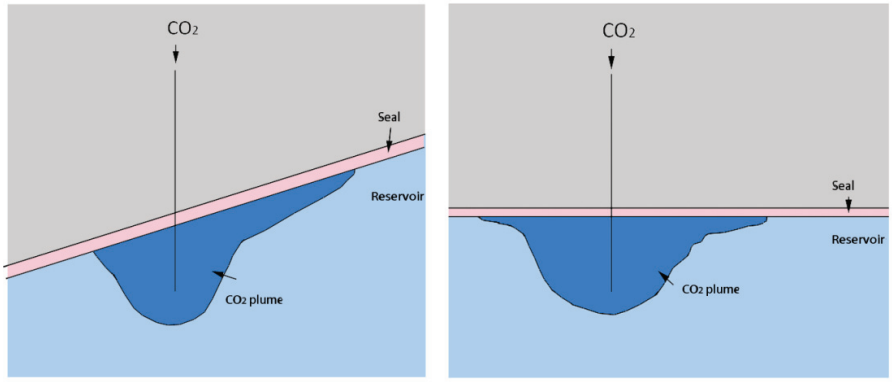

Figure 3 It is possible to trap CO_2 at a large storage site without a closed structure.

On the other hand, CO_2 is also a very good agent for injecting into oil and gas reservoirs to enhance oil and gas recovery by maintaining reservoir pressure. CO_2 injected into the oil reservoir dissolves into the oil and reduces oil density; hence, oil mobility increases considerably. CO_2 could be injected and stored in depleted oil and gas reservoirs where the safety of the trap is relatively certain. In addition, injection of CO_2 to replace the oil and gas removed from depleted oil and gas reservoirs will reduce pressure build-up in the reservoirs. However, there are currently many depleted oil and gas reservoirs available for CO_2 storage that are waiting for actions.

CO_2 trapping mechanisms

Structural/stratigraphic trapping, residual, solution and mineral trapping are four trapping mechanisms known as the main trapping mechanisms of CO_2 in the subsurface porous media (Bachu et al., 2007; Johnson et al., 2004), as shown schematically in Figure 4, from (Wawersik et al., 2001)

.

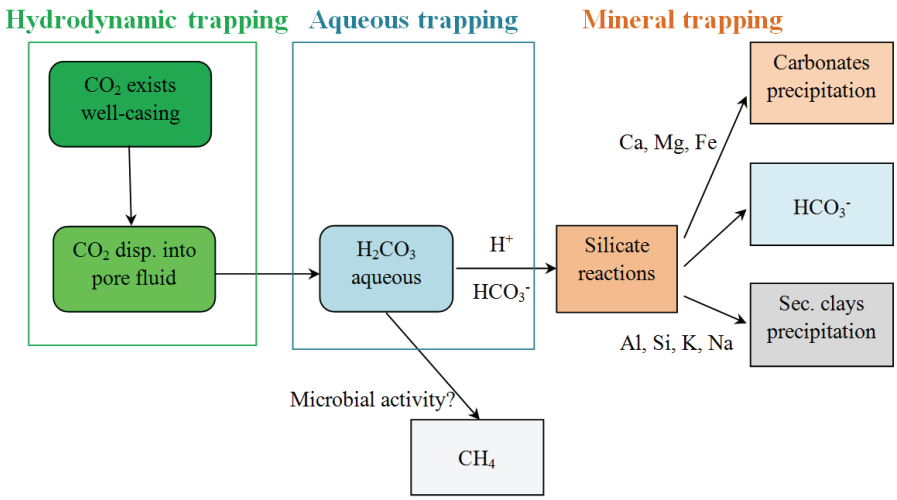

Figure 4. The different phases of CO_2 trapping, from injection where it is trapped in bubbles, then dissolves into the pore water and reacts with the surrounding minerals, to the stable mineralogical form (Wawersik et al., 2001)

The immiscible CO_2 fluid phase, which has been migrating upwards in the reservoir from the injection well, accumulates and is trapped structurally and/or stratigraphically below the seal layer. A part of immiscible CO_2 phase is trapped on its migration way defined as residual fluid CO_2, see figure 5. These two trapping mechanisms together can be designated as hydrodynamic trapping in figure 4. On the other hand, in all parts of the reservoir where fluid CO_2 is in contact with water, part of the CO_2 will also dissolve in the aqueous phase. The amount of dissolved CO_2 will depend on the CO_2 phase pressure (or fugacity), contact area between the CO_2 fluid and water, the time of exposure and accompanying reactions between water and reservoir minerals. The dissolved CO_2 adds carbonic acid to the water and introduces mineral dissolution and precipitation reactions. CO_2 is then trapped in new authigenic minerals. This consumption of CO_2 in the aqueous phase leads to more dissolution of CO_2. Therefore, dissolution trapping (or aqueous trapping) and mineral trapping are intimately connected,

and together may be termed “geochemical trapping” (Gaus et al., 2005b; Johnson et al., 2004; Oelkers et al., 2008).

Structural/stratigraphic trapping and residual trapping could be the most important and dominated mechanisms during injection and the initial storage period. However, solution and mineral trapping mechanisms then become more and more important afterwards and especially in long-term storage. This is shown schematically in Figure 5. Of the four trapping mechanisms, mineral trapping is considered the safest (IPCC, 2005), see Figure 6.

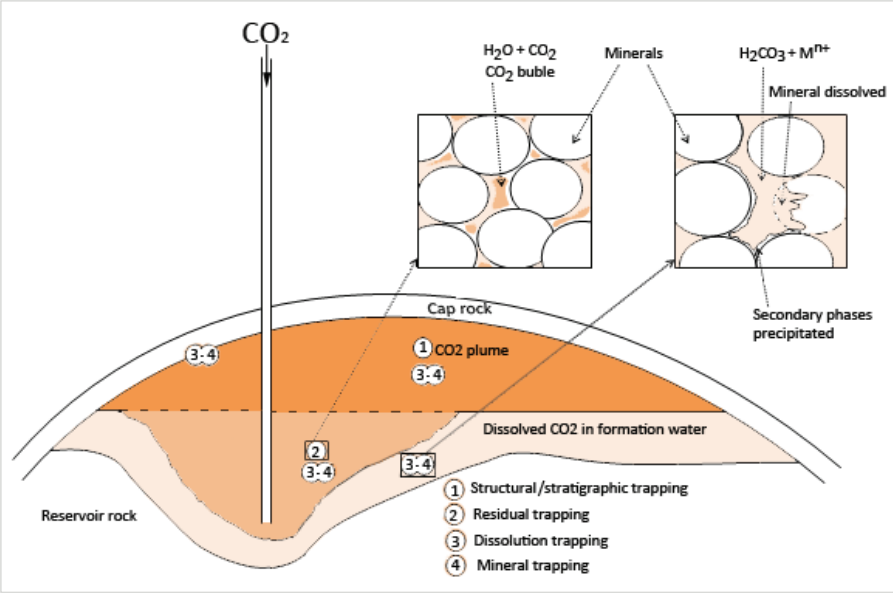

Figure 5 Sketch displaying four trapping mechanisms of CO_2 in a structural trap. M^{n+} represents cations in the solution and n represents the charge of the cations.

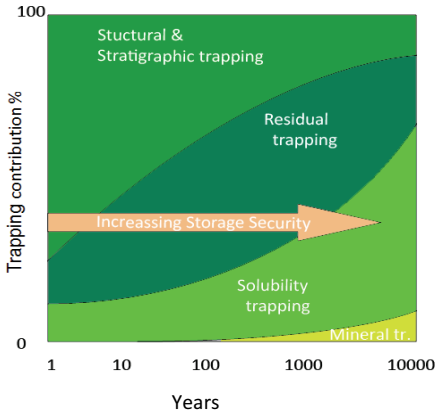

Figure 6 CO_2 storage security depends on a combination of physical and geochemical trapping. Over time, the physical process of residual CO_2 trapping, and geochemical processes of solubility trapping and mineral trapping, increase (IPCC, 2005).

Forecasting storage behavior

The recent industrial storage projects and pilot experiments give valuable information about the short-term storage behavior during injection. The CO_2 injection phase can also build to some degree on experience gained through oil and gas production. However, forecasting the long–term CO_2 storage behavior can only be accomplished by simulation studies. Laboratory studies could be valuable for obtaining essential geochemical and geomechanical properties and parameters, based on these properties and parameters, simulations model can help to predict the complexity of nature, especially in thousands of year.

Simulation studies can help to forecast the behavior of CO_2 in reservoirs and the fraction of each trapping mechanism over time. In this thesis, I have used numerical simulations to investigate other effects in this complex system including geochemical interactions. Examples of the geochemical changes include pH changes, dissolution of the primary minerals in the host rock, precipitation of new phases, and carbonate formation as a result of mineral trapping of CO_2.

1.2 Scientific background

Multiphase flow model

The governing equations in the numerical models used for simulations of geological CO_2 injection and storage are similar to those used to describe oil, water and gas flow through porous reservoirs. Darcy's law, together with equations of conservation of mass and energy are used in the simulations and have recently been reviewed by Jiang (2011). Darcy's equation is described as:

$$\boldsymbol{q} = -\frac{\boldsymbol{k}}{\mu}(\nabla p - \rho g) \quad (1)$$

Where: $\boldsymbol{q}$ is a vector quantity in a three-dimensional (3D) coordinate system representing discharge per unit area, expressed in units of velocity. In Eq. (1), the permeability tensor $\boldsymbol{k}$ represents the ability of the medium to transmit fluids through the pore spaces, μ is the viscosity of the fluid, ∇P is the pressure gradient, ρ is density, and g is gravitational acceleration.

Velocity through the porosity φ of the medium calculated from equation 1:

$$v = \frac{\boldsymbol{q}}{\phi} = -\frac{\boldsymbol{k}}{\mu\phi}(\nabla p - \rho g) \quad (2)$$

For the positive z-direction as vertically up (opposite to gravity), the multi-phase extension of Darcy's law, for an individual fluid phase α, can be given as:

$$v_\alpha = \frac{\boldsymbol{q}_\alpha}{\phi} = -\frac{\boldsymbol{k}k_\alpha}{\mu_\alpha\phi}(\nabla p_\alpha - \rho_\alpha g\nabla z) \quad (3)$$

Where: k_α is the relative permeability of the phase α.

For carbon storage, the flow needs to be modeled as a multi-phase (CO_2, brine, porous solid matrix, etc.) and multi-component (CO_2 and water, etc.) system. The number of phases and components considered can be different depending on the application. In Eq.(4), the conservation of mass is expressed by the balance of four terms representing all the possible mechanisms of mass transfer, which include: 1) the temporal rate of change of mass at a fixed point (or the local derivative or storage term), 2) convective mass transport, 3) diffusive mass transport, and 4) source/sink term for mass. The tortuosity τ refers to the ratio of the diffusivity in the free space to that in the porous medium and is generally larger than unity. The source/sink term S_i in the mass conservation equation represents geochemical reactions.

$$\underbrace{\frac{\partial}{\partial t}\left[\phi\sum_\alpha(\rho_\alpha s_\alpha X_i^\alpha)\right]}_{\text{Storage term}} + \underbrace{\sum_\alpha \nabla(\rho_\alpha X_i^\alpha \boldsymbol{q}_\alpha)}_{\text{Convective transport term}} - \underbrace{\sum_\alpha \nabla(\phi s_\alpha \tau_\alpha D_\alpha \rho_\alpha \nabla X_i^\alpha)}_{\text{Diffusive transport term}} = \underbrace{S_i}_{\text{Souce term}} \quad (4)$$

Where: s_α is saturation of the α phase, X_i is the mole fraction of component *i, and D* is diffusivity.

Capillary force (P_c) is a pressure difference between the non-wetting phase (P_n) and the wetting phase (P_w) in the porous medium. Capillary forces (P_c) are important both in correlated structural/stratigraphic and residual trapping. In the cap-rock (or the seal) the capillary force threshold is high enough to keep the non-wetting (for example gas phase or CO_2 fluid) from entering though the small pore throat in the cap-rock.

$$P_c = P_n - P_w \quad (5)$$

Capillary forces will also keep small bubbles of CO_2 phase immobile in small pore-spaces of the reservoir during migration of CO_2. This phenomenon is defined as residual trapping (Figure 5).

Table 2 Overview of the simulators for geological carbon storage modified from (Jiang, 2011).

Simulators	Main applications	Numerical features (methods for discretisation/integration)
ATHENA/ ACCRETE	Thermal multiphase 3D –reactive-transport numerical code	Finite volume method, reaction and flow iteratively coupled
CHILLER (companion to SOLVEQ)	Multi-component multi-phase equilibrium geochemical calculation software based on minimum free-energy	Newton–Raphson method for solving a system of mass balance and mass action equations
CODE-BRIGHT	Solution of the flow, heat and geo-mechanical model equations	Finite element method for spatial discretisation; implicit finite-difference for temporal discretisation
COORES	Multi-component three-phase and 3D fluid flow in heterogeneous porous media	Finite volume method for spatial discretisation; implicit temporal discretisation
DUMUX	Multi-scale multi-physics toolbox for the simulation of flow and transport processes in porous media	Vertex-centered finite volume method for spatial discretisation; implicit temporal discretisation
ECLIPSE 100/300	Three-phase and 3D fluid flow in porous media with cubic EOS, pressure dependent permeability values, etc.	Integrated finite difference method (IFDM) with irregular spatial discretisation; implicit temporal discretisation
ELSA	Semi-analytical tool to estimate fluid distributions and leakage rates involving vertically integrated sharp-interface equations and local 3D well models	Spatial discretisation is essentially grid free; several schemes for temporal discretisation including implicit pressure explicit saturation, etc.
FEFLOW	Solving the groundwater flow equation with mass and heat transfer, including multi-component chemical kinetics	Finite element method for spatial discretisation; implicit/explicit/Crank–Nicolson temporal discretisation
FEHM	Fully coupled heat, mass and stress balance equations for 3D, non-isothermal, multi-phase fluid flow in porous media	Control volume finite element method for spatial discretisation; implicit temporal discretisation
GEM	EOS compositional reservoir simulator	IFDM for spatial discretisation; implicit temporal discretisation
Geochemist's workbench	Interactive aqueous geochemistry tools	Equilibrium modeling, reaction path modeling calculations, etc.
IPARS-CO_2	Parallel multi-block, multi-physics approach for multi-phase flow in porous media	Mixed finite element method for space discretisation; implicit pressure, explicit concentration sequential algorithm for temporal discretisation
MIN3P	Multi-component reactive transport modeling in variably saturated porous media	Finite volume method for spatial discretisation; implicit temporal discretisation
MODFLOW	Solving the groundwater flow equation to simulate the flow through aquifers	Finite difference method for spatial discretisation; implicit or Crank–Nicolson for temporal discretisation
MT3DMS	Modular 3D transport model simulating convection, dispersion, and chemical reactions of dissolved constituents	Finite difference/particle-tracking based Eulerian–Lagrangian/finite-volume method for spatial discretisation; implicit/explicit temporal discretisation
MUFTE	Isothermal and non-isothermal multi-phase flow problems including compositional effects	Vertex-centred finite volume method for spatial discretisation; implicit temporal discretisation
PFLOTRAN	Parallel 3D reservoir simulator for subsurface multi-phase, multi-component reactive flow and transport based on continuum scale mass and energy conservation	Finite element method for spatial discretisation; implicit/semi-implicit time integration

PHAST	Simulating groundwater flow, solute transport, and multi-component geochemical reactions	Finite difference method for spatial discretisation; implicit or Crank–Nicholson for temporal discretisation
PHREEQC	Low-temperature aqueous geochemical simulator	Based on an ion-association aqueous model; chemical equilibrium, kinetic, transport, and inverse-modeling calculations
RETRASO-CODE Bright	Reactive transport of dissolved and gaseous species in non-isothermal saturated or unsaturated problems, geomechanics	Direct substitution approach for solving the reactive transport equations
ROCKFLOW	Multi-phase flow and solute transport processes in porous and fractured media	Finite element method for spatial discretisation; implicit temporal discretisation
RTAFF2	2D/3D non-isothermal multi-phase and multi-component flow	Finite element method for spatial discretisation; implicit temporal discretisation
SUTRA	Fluid movement and transport of either energy or dissolved substances in a subsurface environment	Hybrid finite element and integrated finite difference method for spatial discretisation; implicit temporal discretisation
TOUGHREACT + TOUGH2	Chemically reactive multi-component, multi-phase, non-isothermal flows in porous and fractured media	IFDM for spatial discretisation; implicit temporal discretisation

'All simulation models are dependent on the types of numerical methods used to translate the governing equations into a finite form, appropriate for computational manipulation and analysis. All of these methods have been used in the available simulators for carbon storage, which are wide ranging in terms of the physical models considered and numerical methods used. Table 2 shows the main features of some available packages/simulators for geological carbon storage, and the complexity of the simulators depends heavily on the number of fluid phases and the number of components considered, as well as the discretization methods used' (Jiang, 2011).

From fluid-flow simulation results, the behavior and distribution pattern of CO_2 in a core-scale model (Basquet et al., 2008) and in field-scale models e.g. of the Utsira and Jonhansen saline aquifers, have been forecasted and described (Audigane et al., 2007; Eigestad et al., 2009; Lindeberg and Bergmo, 2003; Lindeberg et al., 2001; Singh et al., 2010). There are also some other studies in Casablanca (Fornel and Vallaure, 2009) and for a sandstone formation in Gulf Coast aquifers of the United States (Xu et al., 2007).

Injected CO_2 plume distribution was calibrated against 4D-seismic data in Utsira, from the Sleipner platform (Lindeberg et al., 2001; Singh et al., 2010). Very useful information was gained on CO_2 site characterization and monitoring from operational experience at Sleipner, Snøhvit and In Salah, as reported in Eiken et al. (2011) and Hermanrud et al. (2009). At Sleipner, a set of repeated 3D seismic surveys has been reported as well as a set of monitoring data on CO_2 plume distribution based on highly-reflective layers (Figure 7) (Eiken et al., 2011). In addition, satellite monitoring techniques were used to monitor elevation of the ground surface in the In Salah field (Vasco et al., 2010).

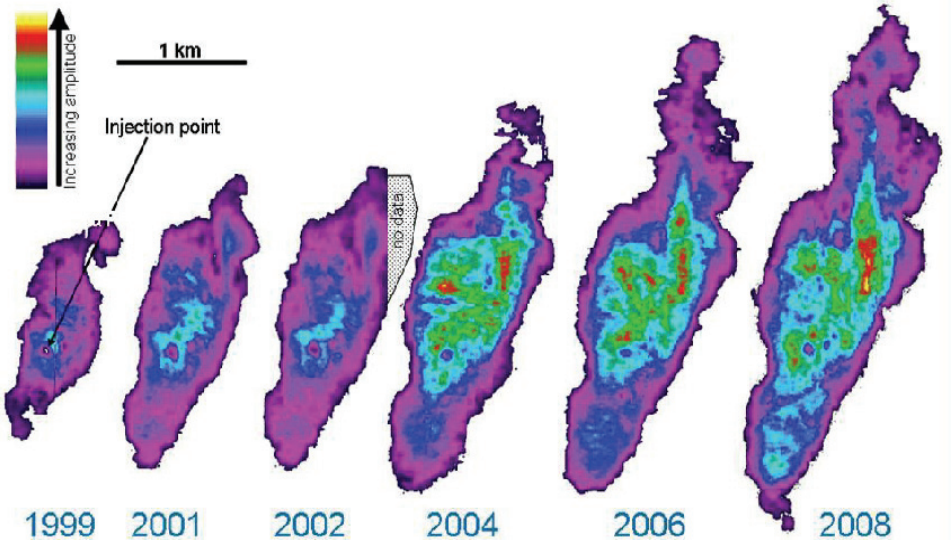

Figure 7 Time-lapse seismic difference reflection amplitude maps at Sleipner, cumulative for all layers. Expansion of the plume in all directions is observed, as well as intensified reflections in the central part of the plume (Eiken et al., 2011).

In a field-scale model, a very fined-scale geological grid model leads to difficulty in calculation and will slow down computer time. Upscaling is a necessary technique for assigning a property value to the cells in order to simplify the process of generating properties from a model. Each cell with field-scale dimensions (for example 100×100×20m) can have only one value based on the averaging of all values in the cell. Using averaging methods with each property to obtain a good representative average value for each cell is very important in the process of generating a 3D grid.

The trapped gas saturation was quantified in an earlier study to be in the range of 24.8 to 28.2%. With the variation in CO_2 density, viscosity and interfacial tension, the Suekane concluded that at least 38.8% of the CO_2 would be stored by residual gas and solubility trapping (Suekane et al., 2008).

CO_2-water-rock interactions and the potential for carbonate mineral formations

Separate phase CO_2 fluid will dissolve into formation water at any location where CO_2 is in contact with an aqueous phase. In most geochemical simulations, it is assumed that dissolved CO_2 (i.e. H_2CO_3, carbonic acid) is in equilibrium with the CO_2 fluid, according to equation (11):

$$CO_2 + H_2O = H_2CO_3 \quad ; K_H \tag{11}$$

Here, K_H is the Henry law constant for the reaction, which is a function of temperature and pressure. We applied the data given by Spycher (2003) and Spycher & Pruess (2005), and calculated the solubility of CO_2 for a wide range of temperature (12 ^oC - 100 ^oC) and pressure ((1 - 600 bars) and salinities in the formation water.

The carbonic acid is a diprotonic acid, with the following dissociation reactions:

$$H_2CO_3 = HCO_3^- + H^+ \qquad K_1 \qquad (12)$$

$$HCO_3^- = H^+ + CO_3^{2-} \qquad K_2 \qquad (13)$$

The acid provides protons, thereby promoting the reactions that dissolve reservoir minerals (exemplified by glauconite dissolution in equation 14). Such reactions consume carbonic acid and lead to higher total inorganic carbon in the formation water, thus increasing solution trapping.

$$Ca_{0.02}K_{0.85}Fe_{1.03}Mg_{1.01}Fe_{0.05}Al_{0.32}Si_{3.735}O_{10}(OH)_2 + 7.06H^+ =$$

$$0.02Ca^{2+} + 0.85K^+ + 1.03Fe^{3+} + 1.01Mg^{2+} + 0.05Fe^{2+} + 0.32Al^{3+} + 3.735SiO_2 + 4.53H_2O \quad (14)$$

The dissolution of primary reservoir minerals will eventually make the formation water supersaturated with respect to various carbonate and aluminosilicate minerals and may lead to precipitation of secondary minerals. Typical clay minerals and carbonates will form, exemplified by calcite formation as shown in equation 15:

$$Ca^{2+} + CO_3^{2-} = CaCO_3 \qquad (15)$$

The combined effect of dissolving CO_2 in formation water and the subsequent mineral-water reactions is to increase both solution and mineral trapping with time.

Modeling of the geochemical processes involved in the storage of CO_2 is a prerequisite for being able to forecast the fate of CO_2 in long-term storage. The source/sink terms in the conservation equations of mass (Eq. 4) are attributed to the chemical processes occurring between formation water and minerals. For instance, the source/sink term (S_i) for the mass of the *i* species can be given as (Jiang, 2011):

$$S_i = \sum_m v_{i.m} \frac{dn_m}{dt} \qquad (16)$$

Where: the sum is over all mineral reactions *m, v* is the stoichiometric amount of element *i* in mineral *m,* and *n* denotes mass of mineral *m.*

The kinetic rate may be modeled using a semi-empirical Arrhenius-type general equation (Aagaard and Helgeson, 1982; Lasaga, 1984), given by:

$$\frac{dn_m}{dt} = k_m A_m \exp\left(\frac{E_{a,m}}{RT}\right)\left\{1 - \left(\frac{Q}{K}\right)_m\right\} \qquad (17)$$

Where: k is the rate constant for the chemical reaction, A is the reaction surface area, E_a is apparent activation energy, R is the universal gas constant, T is temperature, Q is the ion activity product, and K is the equilibrium constant.

Information about the potential for mineral carbonation during CO_2 storage is available from 1) natural systems where CO_2 has reacted with the minerals over extended periods of time (Flaathen et al., 2009; Gaus et al., 2005b; Moore et al., 2005; Pauwels et al., 2007; Worden, 2006), 2) numerical simulations of a range of systems (e.g., André et al., 2007; Cantucci et al., 2009; Gaus et al., 2005a; Gysi and Stefansson, 2008; Hellevang et al., 2009; Johnson et al., 2004; Johnson et al., 2005; Knauss et al., 2005; Xu et al., 2004; Xu et al., 2007), 3) field-scale test-sites (Assayag et al., 2009; Raistrick et al., 2009), and 4) laboratory experiments on mineral dissolution and precipitation (e.g., Declercq et al., 2009; Gislason and Oelkers, 2003; Hellevang et al., 2005; Ketzer et al., 2009; Pokrovsky et al., 2009;

Saldi et al., 2009). Because natural mineral conversion rates are slow relative to laboratory time scales, the best information on the long-term interactions between CO_2-charged waters and minerals might be available from natural analogues. The natural analogues to a silicate reservoirs, e.g. the North Sea Jurassic Sleipner West gas condensate field (Ranaweera, 1987), the Upper Jurassic sandstones of the Magnus field (Baines and Worden, 2004; Macaulay et al., 1993), the Ladbroke in Australia (Watson et al., 2004) and the Montmiral CO_2 accumulation in France (Pauwels et al., 2007), show that the types of carbonate minerals that typically formed were dolomite and ankerite.

In cold siliciclastic reservoirs like the Utsira Sand, where CO_2 has been injected since 1996, there has been no sampling of formation water or observations of the mineral alteration after the CO_2 injection. Previous numerical simulations of CO_2 storage in the Utsira Sand or other similar siliciclastic reservoirs suggested that carbonate minerals such as dawsonite, dolomite, siderite and magnesite may form (Audigane et al., 2007; Gaus et al., 2005a; Johnson et al., 2004; Johnson et al., 2005; Xu et al., 2004). There is much uncertainty, however, in the predictions of the amount and composition of the carbonate assemblage that was expected to precipitate. For some carbonate minerals, like dawsonite and magnesite, the numerical simulations may have overestimated the amounts that forms compared to the what is observed in natural analogues (Haszeldine et al., 2005; Hellevang et al.(write authors' names in refs), 2009).

The conventional method of modeling mineral reaction rates assumes that parameters like the reaction rate coefficients and activation energies are constants that are independent of the affinity of the reaction. Using the transition-state-theory (TST)-based rate law and the principle of detailed balancing from Aagaard and Helgeson (1982) and Lasaga (1984), this assumption leads to very high precipitation rates even at low levels of super-saturation (Hellevang et al., 2009). Comparisons of recent experiments on magnesite and dolomite dissolution and precipitation rates strongly suggest that growth rates even at low levels of super-saturation may be orders of magnitude lower than predicted through TST at corresponding dissolution rates (Pokrovsky et al., 2009; Saldi et al., 2009). Precipitation rates of disordered dolomite and magnesite at the same temperature are in practice zero (Arvidson and MacKenzie, 1997; Saldi et al., 2009). Moreover, the first order dependence on saturation state used for dissolution does not fit with the second order dependence of precipitation observed from the magnesite data of Saldi et al. (2009) or the higher order dependence seen for dolomite (Arvidson and Mackenzie, 1997). Similarly as with magnesite, experiments on dawsonite show fast dissolution rates down to room temperatures (Declercq et al., 2009), whereas dawsonite precipitation is slow even in highly supersaturated solutions at temperatures of 75˚ to 90ºC (Duan et al., 2005).

Carbon dioxide storage research has so far focused mainly on sedimentary basins, but the potential for mineral trapping in basalts and ultra-mafic rock has recently raised interest. Mineral storage of CO_2 in basaltic rock, such as the Colombia River Basalt, may be favored over siliciclastic reservoirs both due to the higher abundance of divalent metal ions in basalt and the faster reactivity of basaltic glass or crystalline basalt (Oelkers et al., 2008).

The basalts often consist of a mixture of glass and crystalline basalt (Schaef and McGrail, 2009; Schaef et al., 2009; Schaef et al., 2010). The alteration process of basalts in natural analogues and the secondary mineral assemblages that form provide valuable information for simulations of CO_2-water-basalt interaction (Neuhoff et al., 1999; Neuhoff et al., 2006; Reidel et al., 2002; Stefansson et al., 2001). For basaltic rocks, aqueous solution species sampled from natural cold springs and rivers at Hekla, Iceland, showed potential formation of secondary carbonate phases like calcite and dolomite (Flaathen et al., 2009). Another natural analogue that more closely corresponds to industrial CO_2

storage is the basalt-hosted petroleum reservoir at Nuussuaq, West Greenland. Here, alteration products such as zeolites and oxides were replaced by dolomite, magnesite, siderite, and calcite at temperatures of 70-120 °C (Rogers et al., 2006). To date, there are not many numerical simulations of CO_2 storage in basaltic rocks other than the simulations of basaltic glass alteration from rain water, river water, and geothermal water, at 25 °C and CO_2 pressures ranging from atmospheric to 30 bars (Gysi and Stefansson, 2008).

An overview of the potential for carbonate formation from a mixture of both basaltic glass and crystalline basalt can be achieved by numerical simulation studies. Furthermore, a numerical model using an improved kinetic rate equation to obtain more accurate results in both basaltic rocks and siliciclastic basins should be considered.

1.3 Scope and Objectives

The research reported in this dissertation addresses several topics that are directly related to CO_2 storage. These include: (1) CO_2-water-rock interactions and the potential for carbonate formation (covered by Papers 1and 2), (2) multiphase flow and CO_2 plume behavior (Paper 3 and extended abstract) and (3) a guide for modeling long-term CO_2-water-rock interactions. The thesis investigates all of the four trapping mechanisms in CO_2 storage: structural/stratigraphic trapping, residual, solution and mineral trapping. No single paper has been able to investigate all of the four trapping mechanisms, but these papers including in the thesis could cover all of the four trapping mechanisms.

Specific objectives:

- To revisit the potential for carbonate growth during CO_2 storage in Utsira-type reservoirs, i.e. low temperature quartz-rich clastic reservoirs, by using an improved geochemical crystal growth model and predicting growth rates more accurately using this modified kinetic equation. Also to explore the level of sensitivity of mineral carbonation to rate parameters such as the reactive surface area for growth, and kinetic parameters affecting nucleation and growth (Paper 1).

- To determine the geochemical potential for secondary carbonate formation in highly reactive basaltic rocks and to estimate the volume changes and the potential for self-sealing following the basalt-CO_2 interactions (Paper 2).

- To simulate CO_2 injection and forecast the behavior and distribution of the CO_2 plume in siliciclastic reservoirs (location chosen is Utsira/Skade aquifer, North Sea, Norway) and to estimate the storage capacity of the reservoir (Paper 3 and extended abstract).

- To propose a guide for long-term numerical modeling of CO_2 storage including geochemical interactions for more complex systems in larger 3D regions using a simplified approach based on the fully kinetic batch simulation (Paper 4).

2. Summary of the papers

The four papers which make up the body of this thesis address related topics on the trapping mechanisms of CO_2 storage. Focusing on the mineral trapping mechanism, Papers 1 and 2 present a geochemical interaction model of CO_2-water-rock and potential carbonate formation in both siliciclastic sandstones and basaltic rock. Focusing on structural, dissolution and residual trapping mechanisms, paper 3 and the extended abstract show a multiphase CO_2 fluid - brine flow model. Paper 4 proposes a guide for long-term numerical modeling of CO2-water-rock interaction. A summary of the papers is presented here.

2.1 CO_2-water-rock interaction & potential carbonate formation (Paper 1-2)

Paper 1: '*On the potential of CO_2-water-rock interactions for CO_2 storage using a modified kinetic model*'. V.T.H. Pham, P. Lu, P. Aagaard, C. Zhu, H. Hellevang. **International Journal of Greenhouse Gas Control 2011,** 5: 1002 - 1015.

In order to study the geochemical reactions of systems having high CO_2 pressures and improve current estimates of the potential for carbonate formation, a modified kinetic model was developed using the Utsira sandstone, Sleipner field as representative of a typical cold and siliciclastic reservoir.

Method:

Because of the flexibility in defining rate equations, PHREEQC was used to model the Sleipner CO_2 storage using a improved kinetic model that takes into accounts both nucleation and growth of secondary mineral phases. The kinetic rate model represented a modification of earlier simulations based on transition state theory, where growth rates were calculated from data on dissolution rate. Because growth rate and nucleation rate parameters were largely unknown for the secondary carbonates, we did a sensitivity study on the potential for carbonate growth on the rate parameters.

Main results and conclusions:

The use of the Transition state theory (TST)-derived equations to predict carbonate growth, using a set of kinetic parameters derived from far-from- equilibrium dissolution rate experiments, leads to considerable overestimation of the growth potential for carbonates such as dolomite, magnesite and dawsonite.

If a mixed-carbonate such as ankerite forms, the long-term potential will be given by the amount of smectite, glauconitic or other reactive clay minerals available in the reservoir, independently of which model were used.

We found that the timing of significant carbonate growth was highly sensitive to nucleation rates. At high nucleation rates, lower super-saturation was required before carbonate phases grew, whereas higher super-saturation was required for growth at low nucleation rates.

It is essential to know the exact composition of the secondary mineral assemblage, in order to understand natural analogues, yet this is dependent on growth and nucleation rate parameters that at present are largely unknown.

There is a great need for experimental data on nucleation and growth of possible secondary minerals like ankerite, siderite and dawsonite.

Paper 2: '*On the potential for CO_2 storage in continental flood basalts*'. V.T.H. Pham, P. Aagaard, H. Hellevang. **Geochemical Transactions 2012, 13: 5.**

The Colombia River Basalt (CRB) is continental flood basalt that is used in this paper to investigate the potential for mineral trapping of CO_2 in basic rocks Basalts are highly reactive and contain an abundance of divalent cations. Basaltic rocks are considered to represent significant potential storage sites in addition to those in sedimentary basins.

Method:

Based on the mineral assemblage and volcanic glass composition of Colombia River Basalt, we estimated the reactive surface of the basalt. The estimate of the reactive surface was based on field data on water composition and the redox stage of the system. It is critical to know the reactive surface in order to calculate the basalt alteration and potential carbonate formation during CO_2 storage.

Kinetic dissolution of primary basalt-minerals (pyroxene, feldspar and glass) and local equilibrium assumption for secondary phases (weathering products) were applied in the simulations using the PHREEQC code.

Main results and conclusions:

Simulations of closed-system (P_{CO_2} = 100 bar, 40 °C) and 1D reaction-diffusion (P_{CO_2} = 0-100 bar, 40 °C) alteration of basalt suggest that the potential of secondary carbonate formation is limited to siderite at low temperatures as divalent metal cations are preferentially consumed by zeolites and oxides. Our simulations on basalt weathering prior to CO_2 injection (low CO_2 pressures) suggest that the main weathering products are zeolites, clays and oxides in low temperature.

Higher temperatures 60 – 100 °C appear to be in favor of secondary carbonate formation, allowing the precipitation of carbonates such as magnesite, siderite and possibly dolomite and other FeMg carbonates (ankerite).

Given an unlimited source of CO_2 (fixed CO_2 pressure), the total amount of CO_2 stored as solid carbonates is orders of magnitude higher than the 1-2 mol/Kg water solubility in the formation water. The total amount trapped might however be reduced if CO_2, H_2O or pore space are limiting factors. The formation of secondary hydrous and carbonate phases increases the volume of solids and the porosity is correspondingly reduced. This together with the immobilization of CO_2 by solid carbonate formation is in favor of safe long-term storage of CO_2 in basaltic aquifers.

Finally, we found that the changes in porosity were varied with temperature and strongly with choice of mineral reactive surface area of the minerals. At high temperature, porosity reduces very quickly while there is a slower decrease at lower temperature. For the base case (10% of the total surface area S_0 reactive) at 40 °C, porosity decreases from 10 % to 1% at the end of 10 000 years. For reactive surface areas defined to be a lower fraction of the total surface, porosity changes are more limited. In the extreme case with a reactive surface area corresponding to the estimated (geometric) total surface area, porosity is clogged after 1000 years.

2.2 Multiphase flow, CO_2 plume behavior and storage capacity (extended abstract + Paper 3)

Extended abstract: '*Numerical modeling including hysteresis properties for CO_2 storage in the Tubåen Formation, Snøhvit Field, Barents Sea'*. V.T.H. Pham, Maast T. E, H. Hellevang, P. Aagaard. **Energy Procedia 2011, 4:** 3746 – 3753.

Method:

An ECLIPSE300 simulator was used and Darcy's flow equation for multiphase fluid flow in a porous medium was applied.

Main results and conclusions:

There was a considerable decrease in the amount of CO_2 injected over the 30 years of injection because of constraints on the bottom-hole pressure that had to be applied to prevent fracturing due to increasing pressure.

The CO_2 plume was distributed over a smaller area in the case where hysteresis properties were applied than in the base case with no hysteresis. The behavior of the reservoir pressure was the same for both.

The CO_2 plume was distributed over a smaller area when diffusion transport was applied than in the case with no diffusion. The reservoir pressure decreased most in the case where diffusion transport was applied.

Paper 3: '*Assessment of CO_2 injection into the south Utsira-Skade aquifer, the North Sea, Norway*.' V.T.H. Pham, I.T. Gjeldvik, F. Riis, E. K. Halland, I. M Tappel, P. Aagaard. **International Journal of Energy (Reviewed January 2013).**

The Utsira Formation and the underlying Skade Formation are considered to be one aquifer and are parts of a large Miocene-Pliocene sandy deltaic complex located in the UK and Norwegian sector in the northern North Sea, covering an area of 450 km north-south and approximately 90 km east-west. To estimate the capacity of CO_2 storage in the Utsira/Skade aquifer, a reservoir model covering 1600 km^2 in the south and located in the Norwegian sector was built to simulate the long-term behavior of CO_2 injection. The objective of the study is to investigate and illustrate potential migration toward the west - the border of Norwegian sector, and in addition, to forecast possible migration of the CO_2 from the Skade Formation into the Utsira Formation above. Different scenarios of the communication between the Skade and Utsira Formations are studied in the reservoir model by varying the transmissibility between them. The simulation model estimated the amount of CO_2 which can be injected into the segment of formations, from that, an overview of storage capacity for the whole area of the aquifer with suitable condition could be estimated.

Method:

The approach of the study was to build geological model and run simulations with using the ECLIPSE300 simulator with CO2STORE module. The modules were used for multiphase in a porous medium and specific for CO_2 storage issue such as CO_2 solubility in brine with different salinity concentration, H_2O solubility in CO_2 phase, and salt precipitation due to water drying out.

Main results and conclusions:

Our simulations show that ca.170 Mt CO_2 could be injected in the segment model with 4 wells in 50 years injection period, BHP change of 10 bars and no water production. The simulation is considered with BHP constraint 10 bars. The CO_2 plume could migrate up to 20 km away from the injection well.

With higher BHP constraint, the maximum storage capacity for the Utsira formation could be higher. The CO_2 plume distribution implied that CO_2 could stay safely in Utsira Formation without migrating up to the area with insufficient seal.

With two different injection targets; Skade and Utsira formations, in Skade formation, it is quite likely that CO_2 could easily migrate up to the depth of -700m in the west due to the tilting of the top Skade surface. In fact, the segment model contacts to the western part of the aquifer at shallow depths. The communicating with the shallow aquifer part on the west causes the CO_2 plume would migrate further to the west, but with less pressure build-up than the results shown in the separate Utsira and Skade base cases.

The simulation results showed that the CO_2 trapped by the dissolution trapping mechanism occupied a fraction of approximately 20 % of the injected CO_2. CO_2 trapped in the residual trapping mechanism was ca. 3 % and CO_2 trapped in the structural/ stratigraphic trapping mechanism more or less 77 % at the end of 50 years of injection. After about 8000 years after the injection period, the dissolved amount increase to nearly 70%, and residual trapping decreases to approximately 1%, while, mobile CO_2 decreased down to 29% of the total CO_2 amount injected. These results were obtained by applying with residual saturation of CO_2 equal to 0.02. Thus, CO_2 residual trapping is 3% (at the end 50 years of injection) and decreasing to 1% after 8000 years. However, if residual saturation of CO_2 equals to 0.3, the CO_2 trapped by residual mechanism will be higher, 35% (at the end 50 years of injection) and decreasing to 13% after 8000 years.

2.3 Kinetic modeling of CO_2-water-rock interactions (Paper 4)

Paper 4: '*Kinetic modeling of CO_2-water-rock interactions*'. H. Hellevang, **V.T.H. Pham**, P. Aagaard. **International Journal of Greenhouse Gas Control (Accepted for publication, 2013**)

The objective of this study is to guide modelers about how to reduce the complexity of geochemical calculations in numerical-simulation models, while still taking account of the most important geochemical reactions occurring in the geological system. This will lead to a reduction in computer time. The study uses the Sleipner-Utsira case as its bench-mark.

Method:

The PHREEQC code was used to run complete kinetic batch simulations in order to rank the most important geochemical reactions in the base case (the Sleipner-Utsira case). The complexity of the model was reduced by removing the less important components and reactions. Finally, the kinetic reactions were approximated using simple analytical expressions for the reactions to be used in the geochemical part of the larger 3D reactive transport models.

Main results and conclusions:

It is challenging to successfully model mineral reactions and formation water changes induced by CO_2 injection, for several reasons. First, quality thermodynamic and kinetic data for some of the reactions can be difficult to obtain; second, no single simple mathematical expression exists that can accurately predict both dissolution and growth rates; and finally, it may cost too much CPU time to solve the full set of geochemical reactions for large-scale reservoir- or basin-scale simulations.

We showed that when the model uses thermodynamic and kinetic data, the largest difficulty is obtaining parameters for mineral nucleation and growth. Growth rate data exist for secondary carbonates such as dolomite and magnesite, but the onset of growth is still difficult to predict because nucleation rate data are scarce. We showed, further, that the common way of modeling mineral growth by extrapolating growth rates from dissolution rate data using transition state theory and the law of mass action may lead to gross over-predictions of growth rates. We have therefore suggested defining separate mathematical expressions for dissolution and growth, and defined a nucleation rate term to generate surface area for the growth of secondary phases.

Finally, we suggested a stepwise procedure for modeling long-term CO_2-water-rock interactions. The first step in this procedure was to identify the significant geochemical reactions by solving the full system of mineral reactions constrained by kinetic expressions. Further steps were suggested in order to simplify the system of geochemical reactions, ultimately leading to analytical expressions, to allow reactions to be included in large-scale reservoir- or basin-scale simulations.

3. General Conclusions

- Flow simulation models are very important for forecasting the behavior and distribution of a CO_2 plume in the reservoir rock. Geological knowledge, rock and fluid properties such as porosity, data on the permeability and relative permeability curves of the water and immiscible CO_2 phases present are all very important and have considerable influence on the results of the model.

- The flow simulation estimated that after ca. 8000 years, the CO_2 trapped by the mechanism of dissolution trapping occupied a large fraction of the injected CO_2 approximately 70 %, assuming that mineral trapping is zero. CO_2 trapped by the residual trapping mechanism is ca. 1 % to 3% (with residual saturation of CO_2 from 0.02 to 0.3) and the CO_2 trapped by the mechanism of structural/ stratigraphic trapping is ca. 29 %.

- A commercial CO_2 storage project often requires an injection rate that is high enough to obtain a designated CO_2 injection volume. High injection rates and CO_2 volumes intended for injection may exceed the injectivity of the reservoir and causing excessive pressure build-up

and geomechanical problems during injection. Compartmentalization and low permeability are the main reasons for the low injectivities. The Snøhvit field is an example of this.

- The problem is not seen in Utsira/ Skade sand because of good quality reservoir. High porosity and permeability, and not least large lateral extent of the aquifer ensure high injectivity and large storage potential.

- The results of the reactive model showed that the potential of CO_2 trapped in solid mineral phases is significant and the CO_2 fraction that could be transferred into minerals is not small over the 10 thousand year time-frame, both in Utsira-type rock and in the Colombia River Basalt. Compared to solubility trapping, even quartz rich reservoirs such as the Utsira sands, with a small fraction of ferro-magnesium rich clay minerals, has a considerable potential to store CO_2 as carbonates.

- Experimental data on the nucleation and growth of possible secondary minerals are very important and necessary for obtaining more accurate results. The simulations in the sedimentary basin also showed that the carbonate potential could be determined by the amount of smectite and glauconite or the other reactive clay minerals available in the reservoir.

References

Aagaard, P., Helgeson, H.C., 1982. Thermodynamic and kinetic constraints on reaction rates among minerals and aqueous solutions I. Theoretical considerations. American Journal of Science, 282: 237-285.

André, L., Audigane, P., Azaroual, M., Menjoz, A., 2007. Numerical modeling of fluid-rock chemical interactions at the supercritical CO_2-liquid interface during CO_2 injection into a carbonate reservoir, the Dogger aquifer (Paris Basin, France). Energy Conversion and Management, 48(6): 1782-1797.

Arvidson, R.S and MacKenzie, F.T., 1997. Tentative kinetic model for dolomite precipitation rate and its application to dolomite distribution. Aquatic Geochem, 2:259-276

Assayag, N., Matter, J., Ader, M., Goldberg, D., Agrinier, P., 2009. Water-rock interactions during a CO_2 injection field-test: Implications on host rock dissolution and alteration effects. Chemical Geology, 265(1-2): 227-235.

Audigane, P., Gaus, I., Czernichowski-Lauriol, I., Pruess, K., Xu, T., 2007. Two-dimensional reactive transport modeling of CO_2 injection in a saline Aquifer at the Sleipner site, North Sea. American Journal of Science, 307(7): 974-1008.

Aziz, K., Settari, A., 1979. Petroleum reservoir simulation. Applied Science in London.

Bachu, S. et al., 2007. CO_2 storage capacity estimation: Methodology and gaps. International Journal of Greenhouse Gas Control, 1(4): 430-443.

Bachu, S., Gunter, W.D., 2004. Acid-gas injection in the Alberta basin, Canada: a CO_2-storage experience. Geological Society, London, Special Publications, 233(1): 225-234.

Baines, S.J., Worden, R.H., 2004. The long-term fate of CO2 in the subsurface: natural analogues for CO_2 storage. Geological Society, London, Special Publications, 233(1): 59-85.

Basquet, R., Rennan, L., Ringen, J.K., Wennberg, O.P., 2008. Fluid flow simulation on core samples containing natural fractures and stylolites. Spe Reservoir Evaluation & Engineering.

Biddle, K.T., Wielchowsky, C.C., 1994. Hydrocarbon traps. In: Magoon, L.B., Dow, W.G. (Eds.), The petroleum system - from source to trap. AAPG Memoir, pp. 219-235.

Bouquet, S., Grendrin, A., Labregere, D., Le Nir, I., 2009. CO2CRC Otway Project, Australia: Parameters Influencing Dynamic Modeling of CO_2 Injection into a Depleted Gas Reservoir. Society of Petroleum Engineers, SPE.

Cantucci, B., Montegrossi, G., Vaselli, O., Tassi, F., Quattrocchi, F., Perkins, E.H., 2009. Geochemical modeling of CO_2 storage in deep reservoirs: The Weyburn Project (Canada) case study. Chemical Geology, 265(1-2): 181-197.

Declercq, J., Hellevang, H., Aagaard, P., 2009. Dawsonite dissolution rate and mechanism at acidic and basic pH; implication for CO_2 storage. submitted to Oil & Gas Science and Technology - Rev. IFP.

Drucker, D.C., Prager, W., 1952. Soil Mechanics and Plastic Analysis or Limit Design. Quarterly of Applied Mathematics, 10(2): 157-165.

Duan, R., Carey, J.W., Kaszuba, J.P., 2005. Mineral chemistry and precipitation kinetics of dawsonite in the geological sequestration of CO_2. American Geophysical Union, Fall Meeting 2005, abstract GC13A-1210.

Eigestad, G.T., Dahle, H.-K., Hellevang, B., Riis, F., Johansen, W.T., and Øian, E., 2009. Geological modeling and simulation of CO_2 injection in the Johansen formation. Computational Geosciences, 13(4): 435-450.

Eiken, O., Ringrose, P., Hermanrud, C., Nazarian, B. and Torp, T., 2011. Lessons learned from 14 years of CCS operations: Sleipner, In Salah and Snøhvit. Energy Procedia, 4: 5541-5548.

Estublier, A., Lackner, A.S., 2009. Long-term simulation of the Snohvit CO_2 storage. Greenhouse Gas Control Technologies 9, 1(1): 3221-3228.

Flaathen, T.K., Gislason, S.R., Oelkers, E.H., Sveinbjörnsdóttir, Á.E., 2009. Chemical evolution of the Mt. Hekla, Iceland, groundwaters: A natural analogue for CO_2 sequestration in basaltic rocks. Applied Geochemistry, 24(3): 463-474.

Flett, M. Brantjes, J., Gurton, R., McKenna, J., Tankersley, T. and Trupp, M. 2009. Subsurface development of CO_2 disposal for the Gorgon Project. Energy Procedia, 1(1): 3031-3038.

Flett, M., Gurton, R., Weir, G., 2007. Heterogeneous saline formations for carbon dioxide disposal: Impact of varying heterogeneity on containment and trapping. Journal of Petroleum Science and Engineering, 57(1-2): 106-118.

Fornel, A., Vallaure, T., 2009. Modeling of CO_2 storage and long term behaviour in the Casablanca field. Energy Procedia, 1(1): 2919-2927.

Gaus, I., Azaroual, M., Czernichowski-Lauriol, I., 2005a. Reactive transport modeling of the impact of CO_2 injection on the clayey cap rock at Sleipner (North Sea). Chemical Geology, 217(3-4): 319-337.

Gaus, I., Le Guern, C., Pauwels, H., Girard, J.-P., Pearce, J., Shepherd, T., Hatziyannis, G., Metaxas, A., 2005b. Comparison of long-term geochemical interactions at two natural CO_2-analogues: Montmiral (Southeast Basin, France) and Messokampos (Florina Basin, Greece) case studies, Greenhouse Gas Control Technologies 7. Elsevier Science Ltd, Oxford, pp. 561-569.

Gislason, S.R., Oelkers, E.H., 2003. Mechanism, rates, and consequences of basaltic glass dissolution: II. An experimental study of the dissolution rates of basaltic glass as a function of pH and temperature. Geochimica Et Cosmochimica Acta, 67(20): 3817-3832.

Gysi, A.P., Stefansson, A., 2008. Numerical modeling of CO_2-water-basalt interaction. Mineralogical Magazine, 72(1): 55-59.

Haszeldine, R.S. Quinn, O., England, G., Wilkinson, M., Shipton, Z., Evans, J. P., Heath, J., Crossey, L., Ballentine, C.J. and Graham, C.M, 2005. Natural geochemical analogues for carbon dioxide storage in deep geological porous reservoirs, a United Kingdom perspective. Oil & Gas Science and Technology - Rev. IFP, 60(1): 33-49.

Hellevang, H., Aagaard, P., Oelkers, E.H., Kvamme, B., 2005. Can dawsonite permanently trap CO_2? Environ Sci Technol, 39(21): 8281-7.

Hellevang, H., Declercq, J., Aagaard, P., 2009. Why is dawsonite absent in CO_2 charged reservoirs? submitted to Oil & Gas Science and Technology - Rev. IFP.

Hermanrud, C. Andresen, A., Eiken, O., Hansen, H., Janbu, A., Lippard, J., Bolas, HN., Simmenes, T., Teige, G., Ostmo, S., 2009. Storage of CO2 in saline aquifers - lessons learned from 10 years of injection into the Utsira Formation in the Sleipner area. Greenhouse Gas Control Technologies 9, 1(1): 1997-2004.

Holloway, S., 2004. Underground sequestration of carbon dioxide - a viable greenhouse gas mitigation option. Energy, 30(11-12): 2318-2333.

IPCC, 2005. IPCC Special Report on Carbon Dioxide Capture and Storage. Prepared by Working Group III of the Intergovernmental Panel on Climate Change In: Metz, B., Davidson, O., Coninck, H., Loos, M., Meyer, L. (eds.). Cambridge University Press, Cambridge, United Kingdom and New York, NY, USA: 442 pp.

Jiang, X., 2011. A review of physical modeling and numerical simulation of long-term geological storage of CO_2. Applied Energy, In Press, Corrected Proof.

Johnson, J.W., Nitao, J.J., Knauss, K.G., 2004. Reactive transport modeling of CO_2 storage in saline aquifers to elucidate fundamental processes, trapping mechanisms and sequestration partitioning. In: Baines, S.J., Worden, R.H. (Eds.), Geological storage of carbon dioxide. Geological Society, Special Publications, pp. 107-128.

Johnson, J.W., Nitao, J.J., Morris, J.P., 2005. Reactive Transport Modeling of Cap-Rock Integrity During Natural and Engineered CO_2 Storage, Carbon Dioxide Capture for Storage in Deep Geologic Formations, pp. 787-813.

Ketzer, J.M. et al., 2009. Water-rock-CO_2 interactions in saline aquifers aimed for carbon dioxide storage: Experimental and numerical modeling studies of the Rio Bonito Formation (Permian), southern Brazil. Applied Geochemistry, 24(5): 760-767.

Knauss, K.G., Johnson, J.W., Steefel, C.I., 2005. Evaluation of the impact of CO_2, co-contaminant gas, aqueous fluid and reservoir rock interactions on the geologic sequestration of CO_2. Chemical Geology, 217(3-4): 339-350.

Lasaga, A.C., 1984. Chemical-Kinetics of Water-Rock Interactions. Journal of Geophysical Research, 89(Nb6): 4009-4025.

Lindeberg, E., Bergmo, P., 2003. The long-term fate of CO_2 injected into an aquifer. Greenhouse Gas Control Technologies, Vols I and Ii, Proceedings: 489-494.

Lindeberg, E., Zweigel, P., Bergmo, P., Ghaderi, A., Lothe, A., 2001. Prediction of CO2 distribution pattern improved by geology and reservoir simulation and verified by time lapse seismic. Greenhouse Gas Control Technologies: 372-377.

Linjordet, A., Olsen, R.G., 1992. The Jurassic Snohvit Gas-Field, Hammerfest Basin, Offshore Northern Norway. Giant Oil and Gas Fields of the Decade 1978-1988, 54: 349-370.

Macaulay, C.I., Haszeldine, R.S., Fallick, A.E., 1993. Distribution, chemistry, isotopic composition and origin of diagenetic carbonates: Magnus sandstone, North Sea. Journal Sedimentary Petrology, 63: 33-43.

Maldal, T., Tappel, I.M., 2004. CO_2 underground storage for Snøhvit gas field development. Energy, 29(9-10): 1403-1411.

Michael, K. Golab, A., Shulakova, V., Ennis-King, J., Allinson, G., Sharma, S., Aiken, T., 2010. Geological storage of CO_2 in saline aquifers--A review of the experience from existing storage operations. International Journal of Greenhouse Gas Control, 4(4): 659-667.

Moore, J., Adams, M., Allis, R., Lutz, S., Rauzi, S., 2005. Mineralogical and geochemical consequences of the long-term presence of CO_2 in natural reservoirs: An example from the Springerville-St. Johns Field, Arizona, and New Mexico, U.S.A. Chemical Geology, 217(3-4): 365-385.

Neuhoff, P.S., Fridriksson, T., Arnorsson, S., Bird, D.K., 1999. Porosity evolution and mineral paragenesis during low-grade metamorphism of basaltic lavas at Teigarhorn, eastern Iceland. American Journal of Science, 299(6): 467-501.

Neuhoff, P.S., Rogers, K.L., Stannius, L.S., Bird, D.K., Pedersen, A.K., 2006. Regional very low-grade metamorphism of basaltic lavas, Disko-Nuussuaq region, West Greenland. Lithos, 92(1-2): 33-54.

Oelkers, E.H., Gislason, S.R., Matter, J., 2008. Mineral Carbonation of CO_2. Elements, 4(5): 333-337.

Pauwels, H., Gaus, I., le Nindre, Y.M., Pearce, J., Czernichowski-Lauriol, I., 2007. Chemistry of fluids from a natural analogue for a geological CO_2 storage site (Montmiral, France): Lessons for CO_2-water-rock interaction assessment and monitoring. Applied Geochemistry, 22(12): 2817-2833.

Pham, T.H.V., Maast, T.E., Hellevang, H., Aagaard, P., (listed as both 2010 and 2011 in text; make consistent) 2011. Numerical modeling including hysteresis properties for CO_2 storage in Tubåen formation, Snøhvit field, Barents Sea. Energy Procedia, 4: 3746-3753.

Pokrovsky, O.S., Golubev, S.V., Schott, J., Castillo, A., 2009. Calcite, dolomite and magnesite dissolution kinetics in aqueous solutions at acid to circumneutral pH, 25 to 150 °C and 1 to 55 atm pCO_2: New constraints on CO_2 sequestration in sedimentary basins. Chemical Geology, 265(1-2): 20-32.

Raistrick, M., Hutcheon, I., Shevalier, M., Nightingale, M., Johnson, G., Taylor, S., Mayer, B., Durocher, K., Perkins, E. and Gunter, B., 2009. Carbon dioxide-water-silicate mineral reactions enhance CO_2 storage; evidence from produced fluid measurements and geochemical modeling at the IEA Weyburn-Midale Project. Energy Procedia, 1(1): 3149-3155.

Ranaweera, H.K.A., 1987. Sleipner Vest field - Norway, Southern Viking graben, North sea. In: Spencer, A. M. (Editor), Geology of the Norwegian Oil and Gas fields: 253-264.

Reidel, S.P., Johnson, V.G., Spane, F.A., 2002. Natural gas storage in basalt aquifers of the Colombia Basin, Pacific Northwest USA: A guide to site characterization. Report Pacific Northwest National Laboratory; PNNL-13962.

Riddiford, F.A., Tourqui, A., Bishop, C.D., Taylor, B., Smith, M., 2003. A cleaner development: The In Salah Gas Project, Algeria. Greenhouse Gas Control Technologies, Vols I and Ii, Proceedings: 595-600.

Riding, J. B., Czernichowski-Lauriol, I., Lombardi, S., Quattrocchi, F., Rochelle, C. A., Savage, D. and Springer, N., 2003, The IEA Weyburn CO2 Monitoring and Storage Project-the European dimension. In: Gale, J. and Kaya, Y. (Eds) Greenhouse Gas Control Technologies, Volume II. Oxford: Elsevier Science Limited, 1629–1632.

Riding, J.B., 2003. The IEA Weyburn CO_2 Monitoring and Storage Project - The European dimension. Greenhouse Gas Control Technologies, Vols I and Ii, Proceedings: 1629-1632.

Rogers, K.L., Neuhoff, P.S., Pedersen, A.K., Bird, D.K., 2006. CO_2 metasomatism in a basalt-hosted petroleum reservoir, Nuussuaq, West Greenland. Lithos, 92(1-2): 55-82.

Saldi, G.D., Jordan, G., Schott, J., Oelkers, E.H., 2009. Magnesite growth rates as a function of temperature and saturation state. Geochimica et Cosmochimica Acta, 73(19): 5646-5657.

Schaef, H.T., McGrail, B.P., 2009. Dissolution of Columbia River Basalt under mildly acidic conditions as a function of temperature: Experimental results relevant to the geological sequestration of carbon dioxide. Applied Geochemistry, 24(5): 980-987.

Schaef, H.T., McGrail, B.P., Owen, A.T., 2009. Basalt-CO2-H2O Interactions and Variability in Carbonate Mineralization Rates. Greenhouse Gas Control Technologies 9, 1(1): 4899-4906.

Schaef, H.T., McGrail, B.P., Owen, A.T., 2010. Carbonate mineralization of volcanic province basalts. International Journal of Greenhouse Gas Control, 4(2): 249-261.

Singh, V., Cavanagh, A., Hansen, H., Nazarian, B., Iding, M., Ringrose, P., 2010. Reservoir Modeling of CO_2 Plume Behavior Calibrated Against Monitoring Data From Sleipner, Norway. Society of Petroleum Engineers.

Spycher, N., Pruess, K., 2005. CO2-H2O mixtures in the geological sequestration of CO_2 center dot. II. Partitioning in chloride brines at 12-100 degrees C and up to 600 bar. Geochimica Et Cosmochimica Acta, 69(13): 3309-3320.

Spycher, N., Pruess, K., Ennis-King, J., 2003. CO2-H2O mixtures in the geological sequestration of CO_2. I. Assessment and calculation of mutual solubilities from 12 to 100 degrees C and up to 600 bar. Geochimica Et Cosmochimica Acta, 67(16): 3015-3031.

Stefansson, A., Gislason, S.R., Arnorsson, S., 2001. Dissolution of primary minerals in natural waters - II. Mineral saturation state. Chemical Geology, 172(3-4): 251-276.

Suekane, T., Nobuso, T., Hirai, S., Kiyota, M., 2008. Geological storage of carbon dioxide by residual gas and solubility trapping. International Journal of Greenhouse Gas Control, 2(1): 58-64.

Torp, T.A., Gale, J., 2004. Demonstrating storage of CO2 in geological reservoirs: The sleipner and SACS projects. Energy, 29(9-10): 1361-1369.

Van Der Meer, L.G.H., Kreft, E., Geel, C., 2005. K12-B: A Test Site for CO_2 Storage and Enhanced Gas Recovery SPE Europec/EAGE Annual Conference, 13-16 June 2005, Madrid, Spain.

Vasco, D.W., Rucci, A., Ferretti, A., Novali, F., Bissell, R., Ringrose, P., Mathieson, A. and Wright, I., 2010. Satellite-based measurements of surface deformation reveal fluid flow associated with the geological storage of carbon dioxide. Geophysical Research Letters, 37.

Watson, M.N., Zwingmann, N., Lemon, N.M., 2004. The Ladbroke Grove-Katnook carbon dioxide natural laboratory: A recent CO_2 accumulation in a lithic sandstone reservoir. Energy, 29(9-10): 1457-1466.

Wawersik, W.R., Rudnicki, J.W., Dove, P., Harris, J., Logan, J.M., Pyrak-Nolte, L., Orr, F.M., Ortoleva, P.J., Richter, F., Warpinski, N.R., Wilson, J.L., Wong, T.F., 2001. Terrestrial sequestration of CO_2: An assessment of research needs. Advances in Geophysics, Vol. 43, 43: 97-177.

Worden, R.H., 2006. Dawsonite cement in the Triassic Lam Formation, Shabwa Basin, Yemen: A natural analogue for a potential mineral product of subsurface CO_2 storage for greenhouse gas reduction. Marine and Petroleum Geology, 23(1): 61-77.

Xu, T., Apps, J.A., Pruess, K., 2004. Numerical simulation of CO_2 disposal by mineral trapping in deep aquifers. Applied Geochemistry, 19(6): 917-936.

Xu, T., Apps, J.A., Pruess, K., Yamamoto, H., 2007. Numerical modeling of injection and mineral trapping Of CO_2 with H_2S and SO_2 in a sandstone formation. Chemical Geology, 242(3-4): 319-346.

Paper 1

On the potential of CO_2-water-rock interactions for CO_2 storage using a modified kinetic model

By:

V.T.H. Pham, P. Lu, P. Aaagaard, C. Zhu, H. Hellevang.

International Journal of Greenhouse Gas Control (2011), 5: 1002 -1015

Paper 2

On the potential for CO_2 storage in continental flood basalts

By:

V.T.H. Pham, P. Aaagaard, H. Hellevang.

Geochemical Transaction 2012, 13: 5.

Van Pham et al. Geochemical Transactions 2012, 13:5
http://www.geochemicaltransactions.com/content/13/1/5

GEOCHEMICAL TRANSACTIONS
Geochemical Transactions

RESEARCH ARTICLE Open Access

On the potential for CO_2 mineral storage in continental flood basalts – PHREEQC batch- and 1D diffusion–reaction simulations

Thi Hai Van Pham*, Per Aagaard and Helge Hellevang

Abstract

Continental flood basalts (CFB) are considered as potential CO_2 storage sites because of their high reactivity and abundant divalent metal ions that can potentially trap carbon for geological timescales. Moreover, laterally extensive CFB are found in many place in the world within reasonable distances from major CO_2 point emission sources.

Based on the mineral and glass composition of the Columbia River Basalt (CRB) we estimated the potential of CFB to store CO_2 in secondary carbonates. We simulated the system using kinetic dependent dissolution of primary basalt-minerals (pyroxene, feldspar and glass) and the local equilibrium assumption for secondary phases (weathering products). The simulations were divided into closed-system batch simulations at a constant CO_2 pressure of 100 bar with sensitivity studies of temperature and reactive surface area, an evaluation of the reactivity of H_2O in $scCO_2$, and finally 1D reactive diffusion simulations giving reactivity at CO_2 pressures varying from 0 to 100 bar.

Although the uncertainty in reactive surface area and corresponding reaction rates are large, we have estimated the potential for CO_2 mineral storage and identified factors that control the maximum extent of carbonation. The simulations showed that formation of carbonates from basalt at 40 C may be limited to the formation of siderite and possibly FeMg carbonates. Calcium was largely consumed by zeolite and oxide instead of forming carbonates. At higher temperatures (60 – 100 C), magnesite is suggested to form together with siderite and ankerite. The maximum potential of CO_2 stored as solid carbonates, if CO_2 is supplied to the reactions unlimited, is shown to depend on the availability of pore space as the hydration and carbonation reactions increase the solid volume and clog the pore space. For systems such as in the $scCO_2$ phase with limited amount of water, the total carbonation potential is limited by the amount of water present for hydration of basalt.

Introduction

Underground sequestration of carbon dioxide is a potentially viable greenhouse gas mitigation option as it reduces the release rate of CO_2 to the atmosphere [1]. CO_2 can be trapped subsurface by four storage mechanisms: (1) structural and stratigraphic trapping; (2) residual CO_2 trapping; (3) solubility trapping; and (4) mineral trapping [2]. Mineral trapping has been considered as the safest mechanism in long-term storage of CO_2 [3].

Mineral storage of CO_2 in basaltic rocks is favored over siliciclastic reservoirs both by the higher abundance of divalent metal ions in basalt and the faster reactivity of basaltic glass or crystalline basalt [4]. Moreover, basalts such as the Columbia River flood basalts (CRB) are abundant and in many places close to CO_2 point source emissions [5]. During the last decade several flood basalts around the world have been mapped for the possibility of CO_2 storage, and possible candidates such as CRB in USA and the Deccan traps in India have been identified [4-6].

To be a candidate for CO_2 storage, the flood basalt must have a proper sealing and sufficient injectivity, the latter limited by the available connected pore space. In

* Correspondence: vtpham@geo.uio.no
Department of Geosciences, University of Oslo, Pb. 1047, Blindern, Oslo, Norway

flood basalts, the connected pore space is typically found at zones containing abundant vesicles or in breccias between basalt flows. Because central zones of flood basalts commonly are dense and impermeable without vesicles, and flows are laterally continuous over large areas and commonly stacked vertically for hundreds of meters, flow units can act as seals [5]. The non-porous inner parts of flows may however be penetrated by networks of vertical fractures. These fractures can be open and conductive, or closed by mineralization and non-conductive.

The main objectives of this study were to performe batch- and 1D diffusion–reaction numerical simulations to determine the geochemical potential for secondary carbonate formation and to estimate the volume changes and the possibility of self-sealing following the basalt-CO_2 interactions. The CRB system was used as an example case and our results were compared to earlier reported laboratory experiments and numerical simulations of CO_2-basalt interactions. As CO_2 stored underground will distribute spatially in the reservoir to give a range of reactive conditions, such as the potential of reactions by H_2O dissolved in supercritical CO_2 [7,8] or reactions in the H_2O-rich phase from residually trapped CO_2, we divided the simulations into three systems representing different parts of CO_2 storage: (1) basalt alteration in the H_2O-rich phase at constant CO_2 pressure; (2) basalt alteration in a H_2O saturated CO_2 phase, and (3) reactions at the boundary of the CO_2 plume where CO_2 diffuses into the aquifer from the boundary of the CO2 plume (Figure 1).

Methods

All thermodynamic and kinetic calculations were performed using the geochemical code PHREEQC-2 [9]. This code is capable of simulating complex interactions between dissolved gases, aqueous solutions, and mineral assemblages in batch and 1D advection–diffusion-reaction mode. As the code can only model fully saturated systems, natural systems must be simplified to end-member situations, such as given by constant pressure boundary conditions as may be the case close to underground CO_2 plumes, or the assumption of packages (batches) of water reacting along a reaction path with a homogenous sediment or rock body. Based on these limitations we divided the simulations into three systems representing different parts of CO_2 storage: (1) basalt alteration in the H_2O-rich phase at constant CO_2 pressure; (2) basalt alteration in a H_2O saturated $scCO_2$ phase, and (3) reactions at the boundary of the CO_2 plume where CO_2 diffuses into the aquifer from the boundary of the $scCO_2$ plume (Figure 1). In the second case, we assumed that the CO_2 phase had swept through the systems and dried out residual water, giving only dissolved water in the $scCO_2$ phase. In this case an upper limit of carbonation potential was estimated as reactions were allowed to occur until (nearly) all water was consumed, passing the upper 2 mol/Kgw theoretical limit for the Truesdell-Jones activity model [9].

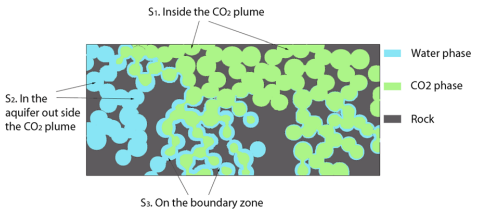

Figure 1 Sketch of possible reaction settings during CO_2 storage in basalt. System 1 (S1) is close to the injector and contains a wet CO_2 (0.5 mole% H_2O at 100 bar and 40 C) with no residual water; system 2 (S2) is fully in the H_2O rich phase with CO_2 diffusing in from the plume boundary; and system 3 (S3) is at the boundary of the CO_2 plume with both sufficient non-wetting CO_2 at a constant CO_2 partial pressure of 100 bar and with sufficient water wetting the mineral surfaces and available for reactions.

The standard state adopted in this study for the thermodynamic calculations was that of unit activity for pure minerals and H_2O at any temperature and pressure. For aqueous species other than H_2O, the standard state was unit activity of the species in a hypothetical 1 molal solution referenced to infinite dilution at any temperature and pressure. For gases, the standard state was for unit fugacity of a hypothetical ideal gas at 1 bar of pressure. All simulations used the llnl.dat database based on the thermo.com. V8.R6.230 dataset prepared at the Lawrence Livermore National Laboratory, with additions of thermodynamic data for those phases not present (see description below).

CO_2 fugacity coefficients were estimated according to the modified Redlich-Kwong (SRK) equation of state [10] and the solubility was adjusted for by a poynting correction term ($exp(v_{CO2}(P_{sat} - P)/RT)$ where v denotes molar volume, P pressure, R the universal gas constant and T absolute temperature) [11]. The density of CO_2 at 40 C and 100 bar was approximated from Bachu and Stewart [12] to be 600 Kg/m^3 and the solubility of water in $scCO_2$ at the same conditions was approximated to 0.5 mole% [13,14]

The simulations were divided into batch simulations of the H_2O rich and CO_2 rich phases respectively, and 1D diffusion of CO_2 in the H_2O rich phase to obtain information on the CO_2-basalt interactions over a continuous range of CO_2 pressures. The latter was solved by PHREEQC using $\partial_t C = D_L \partial_x^2 C + q$, where C denotes molal (mol/Kgw) concentration, q denotes the sink term, subscripts t and x refer to derivatives in time and x-direction respectively, and an efficient diffusion coefficient D_L of 0.45×10^{-9} m^2/s was used for CO_2 [15] and all solutes.

Dissolution rates of minerals in the basaltic rock were calculated according to a kinetic equation taking into account pH and the distance from equilibrium:

$$r_+ = S\left\{k_H exp\left(\frac{-E_{a,H}}{RT}\right)a_H^{n_H} + k_N exp\left(\frac{-E_{a,N}}{RT}\right) + k_{OH} exp\left(\frac{-E_{a,OH}}{RT}\right)a_H^{n_{OH}}\right\}(1-\Omega) \quad (1)$$

where S is the reactive surface area (m^2), k_i are rate constants (moles/m^2s), a_H is the H^+ activity, n is the reaction order with respect to H^+ and OH^-, and Ω is the saturation state given by:

$$\Omega = \exp\left(\frac{\Delta G_r}{RT}\right) \quad (2)$$

Where ΔG_r is the Gibbs free energy of the reaction, R is the gas constant, and T is absolute temperature. Reaction rate constants for crystalline basalt (pyroxenes and plagioclase) were obtained from Palandri and Kharaka [16], and pH dependencies were taken from the same source. The dissolution rate of basaltic glass was calculated according to the expression suggested by Gislason and Oelkers [17]:

$$r_+ = k_+ exp\left(\frac{-E_a}{RT}\right)S\left(\frac{a_{H^+}^3}{a_{Al^{3+}}}\right)^{0.33}(1-\Omega) \quad (3)$$

where k_+ is the far-from-equilibrium dissolution rate coefficient. The saturation state term 1-Ω was approximated to 1 (i.e., rate independent to distance from equilibrium) supported by earlier numerical estimates of glass-CO_2 reactivity suggesting an approximately linear relation between time and reaction progress for basaltic glass [18]. This expression takes into account the effect of pH as well as the effect of the concentration of solutes such as fluoride as they complex with Al^{3+} and reduce the Al^{3+} activity [19]. The specific surface area for basalt (m^2/g) was estimated by:

$$S_{sp} = \frac{\phi}{1-\phi}\frac{A_p}{\bar{\rho}_s V_p} \quad (4)$$

where the ratio A_p/V_p denotes the ratio between pore surface and pore volume (m^{-1}), ϕ is connected porosity, and $\bar{\rho}_s$ (g/m^3) is the density of the basalt solid estimated from the fraction of the individual basalt components. A S_{sp} value of 1.52×10^{-5} m^2/g basalt (= 0.137 m^2/Kg water) was obtained for the CRB using an average basalt solid density of 2.93×10^6 g/m^3 with 10% connected pore space and a A_p/V_p ratio of 400 m^{-1} [5]. The reactive surface area was calculated from the mass of the glass and minerals present according to:

$$S_i = M_i n_i S_{sp} X_r \quad (5)$$

where M and n are molar mass and moles of mineral i, and X_r is the fraction of the total mineral surface that is reactive. As X_r is highly uncertain and is suggested to vary by orders of magnitude [20,21], we used a value of 0.1 for the base case and varied X_r from 1 to 10^{-3}. The use of mass or mass fractions of the individual basalt components to estimate the release rates of elements from the basalt is supported by a recent experimental study which suggests that release rates estimated from the sum of volume fractions of the constituent minerals are within one order of magnitude from measured values [22]. A list of kinetic parameters is given in Table 1. All secondary phases were allowed to form according to the local equilibrium assumption [23].

Changes in solid-phase volumes and porosities ϕ caused by the mineral reactions were calculated according to:

$$\Delta\phi_t = \left(1 - \frac{\sum_i n_{i,t}\bar{v}_i}{V_{total}}\right) - \phi_{t=0} \quad (6)$$

where $\phi_{t=0}$ is the initial porosity, n and $\bar{v}$ are moles and molar volume of mineral i respectively, and V_{total} is the total volume of the system.

The basalt was defined to consist of a mixture of glass and crystalline basalt with mineral and glass fractions chosen based on reported data from CRB [6,24,25]. To represent the crystalline basalt, plagioclase ($Ca_{0.5}Na_{0.5}Al_{1.5}Si_{2.5}O_8$) and the pyroxenes augite ($Ca_{0.7}Fe_{0.6}$ $Mg_{0.7}Si_2O_6$) and pigeonite ($Ca_{1.14}Fe_{0.64}$ $Mg_{0.22}Si_2O_6$) were chosen. The hydrolysis equilibrium constants of these phases were estimated using the PHREEQC program assuming ideal solid solutions of the end-members enstatite, ferrosilite and wollastonite for the pyroxenes, and albite and anorthite for the

Table 1 Kinetic parameters for dissolution of primary minerals based on empirical data given in Palandri and Kharaka [16] and for basaltic glass from [17]

	$k_{\_H}$ (mol/m^2s)	Ea_H kJ/mol	n_H	$k_{\_N}$ (mol/m^2s)	Ea_NkJ/mol	$k_{\_OH}$ (mol/m^2s)	Ea_{OH}kJ/mol	n_{OH}	References
Augite	1.58e-7	78	0.7	1.07e-12	78	-	-		[16]
Pigeonite	1.58e-7	78	0.7	1.07e-12	78	-	-		[16]
Feldspar	1.58e-9	53.5	0.541	3.39e-12	57.4	4.78e-15	59	-0.57	[16]
glass	1e-10	25.5	1	-	-	-	-	-	[17]
Magnetite	2.57e-9	18.6	0.279	1.66e-11	18.6	-	-	-	[16]

plagioclase. Equilibrium constants for the solid solutions for temperatures up to 100 C were estimated with PHREEQC and from these data coefficients *a* to *e* for the PHREEQC built-in analytical expression ($log\ K = a + bT + c/T + dlog_{10}(T) + e/T^2$) were estimated using non-linear regression in MATLAB.

The glass composition ($Ca_{0.015}Fe_{0.095}\ Mg_{0.065}Na_{0.025}\ K_{0.01}Al_{0.105}\ S_{0.003}Si_{0.5}O_{1.35}$) was taken from [6] and modified by adding a small fraction of sulfur which is a common minor constituent of the CR basaltic glass [26].

The secondary mineral assemblage was chosen based on reports on basalt weathering [27-30], with additional carbonates that could potentially form at elevated CO_2 pressures from the release of Fe, Mg and Ca. The ankerite composition chosen for this work was $CaFe_{0.6}\ Mg_{0.4}(CO_3)_2$ which corresponds to a solid solution of 0.6 ankerite ($CaFe(CO_3)_2$) and 0.4 dolomite ($CaMg(CO_3)_2$). Because ankerite ($CaFe_{0.6}\ Mg_{0.4}(CO_3)_2$) was not listed in the thermodynamic database, we estimated values using the same approach as in [31]. The full list of secondary minerals is given in Table 2.

To simulate the CRB-CO_2 interaction we used the average concentrations of solutes reported for the Grand Ronde Formation (Table 3). As supercritical CO_2 ($scCO_2$ at $T > 31.1$ C; $P > 73.9$ bar) is the preferred choice for CO_2 storage, based on higher density compared to gaseous CO_2, we simulated aqueous-phase basalt-CO_2 interaction at a depth of 800 meters at a CO_2 pressure of 100 bar and temperatures of 40 to 100 C. The reactivity of basalt and a H_2O saturated $scCO_2$ phase was simulated using an estimated 0.5 mol% H_2O and a CO_2 density of 600 g/cc giving an initial mass of 0.003 Kg H_2O per 1 liter pore space.

Results

System 1: Basalt alteration in the H_2O-rich phase at constant CO_2 pressure

i) CRB mineral and glass dissolution and formation of secondary minerals

Following the injection of CO_2 into the system, pH immediately decreased from 9.5 to below 4, and thereafter gradually increased to 5.8 at the end of 10000 years (Figure 2a). At the acidic pH secondary phases such as saponite ($Ca_{0.165}Mg_3Al_{0.33}Si_{3.67}O_{10}(OH)_2$), celadonite ($KMgAlSi_4O_{10}(OH)_2$) and zeolite (stilbite) were thermodynamically stable and formed (Figure 2b). Glass dissolved orders of magnitude faster than the crystalline basaltic constituents and more than half dissolved after 10000 years (Figure 2c). The dissolution rate of glass was not increased by the aqueous fluoride as the Al^{3+} activity was fixed by the kaolinite and amorphous silica equilibria. The fluoride therefore only increased the total soluble aluminium. The steady release of Fe from the basalt saturated the water with respect to siderite and a total amount of 10 moles/kgw formed after 10000 years (Figure 2d). Other carbonates, such as ankerite, dolomite, magnesite, and dawsonite did not form as elements such as Mg and Ca was consumed by the non-carbonate secondary phases.

The effect of temperature on the basalt hydration and carbonation was investigated by simulating the system at 60, 80 and 100 C (Figure 3). As for the 40 C simulation we see that basaltic glass dissolves orders of magnitude faster than the crystalline basalt components and the glass is the major source for the secondary phases. The dissolution rates of the basalt components scale exponentially with temperature, and the glass is almost

Table 2 Mineralogy included in the model

	Initial Weight %	Density (g/cm^3)	[2,3]Log K^0
Primary minerals			
[1]Augite (En0.35Fs0.3Wo0.35)	16	3.40	21.00
[1]Pigeonite (En0.57Fs0.32Wo0.11)	3	3.38	21.40
[1]Plagioclase (An50)	35	2.68	14.20
Glass $Ca_{0.015}Fe_{0.095}Mg_{0.065}\ Na_{0.025}K_{0.01}Al_{0.105}\ S_{0.003}Si_{0.5}O_{1.35}$	45	2.92	-99.00
Magnetite	1	5.15	10.47
Secondary minerals			
SiO_2(am)	0	2.62	-2.71
Albite	0	2.62	2.76
Goethite	0	3.80	0.53
Calcite	0	2.71	1.85
Hematite	0	5.30	0.11
Kaolinite	0	2.60	6.81
Smec high Fe-Mg	0	2.70	17.42
Saponite-Mg	0	2.40	26.25
Celadonite	0	3.00	7.46
Stilbite	0	2.15	1.05
Dawnsonite	0	2.42	4.35
Siderite	0	3.96	-0.19
[1]Ankerite ($Ank_{0.6}Do_{0.4}$)	0	3.05	-19.51
Dolomite	0	2.84	4.06
Magnesite	0	3.00	2.29

The mineralogy of the CRB has been described in [25,32] and the weight fraction of pyroxene, feldspar and glass was estimated as average values from the reported data.

[1]Solid solutions. En (enstatite), Fs (ferrosilite), Wo (wollastonite), An (anorthite), Ank (ankerite), Do (dolomite). For details on the calculations of the ankerite solid solution see [31].

[2]Superscript ^{0} denotes Standard state ($T = 298K$, $P = 1$ atm). The equilibrium constant *log K* value is that for the forward dissolution reaction for one mole unit of the mineral.

[3]All thermodynamic data (*log K* and coefficients for the PHREEQC analytical temperature expression) from the llnl.dat PHREEQC database, except for the solid-solutions first estimated in PHREEQC by ideal solid solutions and then added to the PHREEQC database as new solid solution phases.

Table 3 Composition of initial formation water

Elements (totals)	Mol/kgw
Na	1.0×10^{-3}
Ca	6.0×10^{-4}
K	1.0×10^{-4}
Mg	2.0×10^{-5}
Fe	1.2×10^{-6}
Alkalinity (HCO_3^-)	2.0×10^{-3}
Cl	3.0×10^{-4}
S (SO_4^{2-})	1.0×10^{-4}
Si	2.0×10^{-4}
Al	1.0×10^{-6}
Log(O_2)	-10.68
pH	7.5

completely dissolved after 10000 years at 60 C, whereas the time for a complete dissolution takes 4000 and 1500 years at 80 and 100 C respectively (Figure 3a, d, g). The secondary mineral assemblages were largely the same for all temperatures. Stilbite dominated together with amorphous silica (40 and 60 C) and quartz (80 and 100 C) (Figure 3b, e, h). Saponite formed at 40 and 60 C, but not at higher temperatures. Other secondary minerals such as albite, celadonite, and kaolinite formed at all conditions. At 60 C, magnesite and dolomite were still considered to be too slow to form (see [29]) and siderite was the only phase that formed. At 80 and 100 C, magnesite and later ankerite formed together with siderite. Taking zero porosity as the maximum extent of possible reactions we see that the total amount of CO_2 trapped as solid carbonates did not change much with temperature (Figure 4). The reaction rates increased however with temperature and the time needed to reach the maximum potential therefore decreased with temperature (Figure 4).

ii) On the limitation of pore-space for the basalt carbonation

Secondary phases such as stilbite and amorphous silica have lower density than the basalt components and alteration therefore leads to a reduction of pore space. At the presence of CO_2, secondary carbonates further reduce the pore space. For the volume calculations we used expression (6) with the molar volumes listed in Table 2. At 40 C, the starting porosity of 10% is reduced to 0.85% after 10000 years. At the higher temperatures all porosity is lost after 2700, 1200, and 300 years respectively at 60, 80, and 100 C (Figure 5). Taking the extreme of 0% porosity as the limit for the reactions we obtain a maximum carbonation potential (mol CO_2 stored/Kgw) at the different temperatures of 13.5, 29.3, and 28.5 moles for 60, 80, and 100 C (Figure 5). The simulated clogging of the pore space fits well with short-term laboratory percolation experiments on open-system

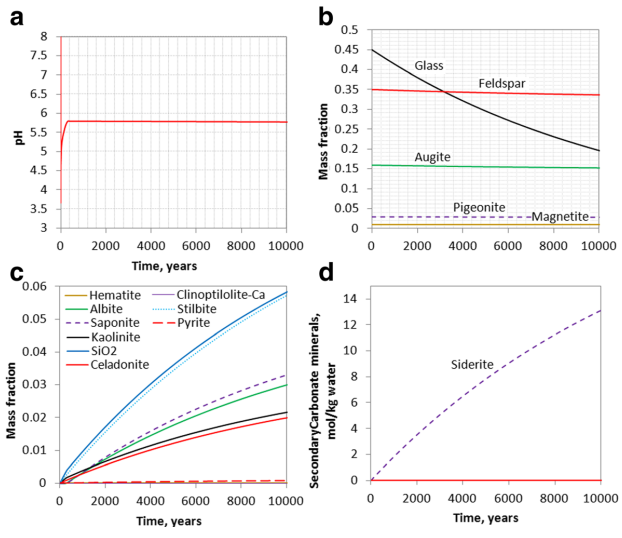

Figure 2 Basalt alteration at 40 C and 100 bar CO_2 pressure over 10000 years. a) pH changes; **b**) mass fractions of basaltic glass and crystalline basalt components; **c**) secondary phases formed; and **d**) moles of secondary carbonates (siderite) formed per kgw.

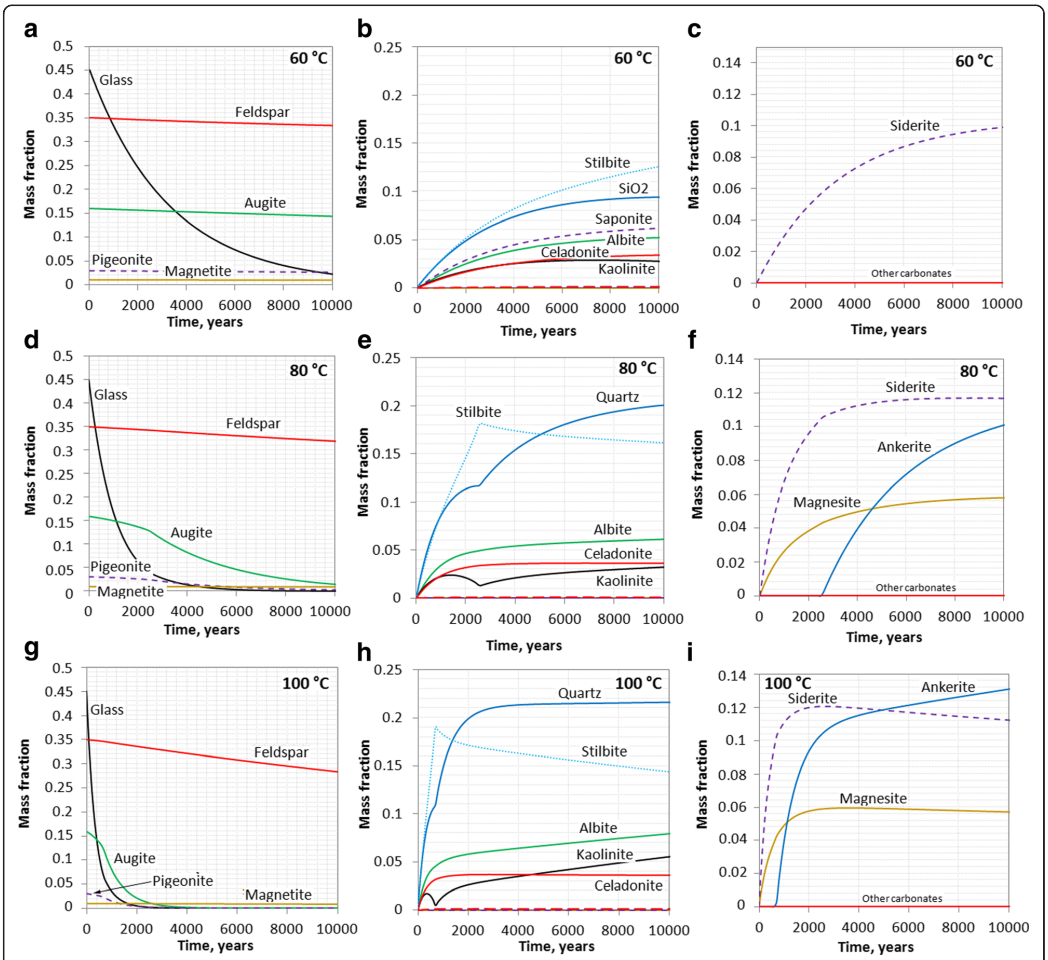

Figure 3 Mass fractions of minerals following basalt alteration at 60, 80, and 100 C over 10000 years: **a**, **d**, **g**) primary basalt minerals and glass; **b**,**e**, **h**) secondary phases except the carbonates; and **c**, **f**, **j**) carbonates.

basalt-CO_2 alteration which shows loss of porosity and a rapid reduction of permeability during CO_2-basalt interactions (e.g., [33]).

iii) Reduction of pore-space as a function of reactive surface area

As the reactive surface area is a large uncertainty we simulated the changes of porosity over a range of values from a maximum being equal to the estimated physical surface area S_0 (equation (5) with $X_r = 1$) to a three orders of magnitude reduction (Figure 6). The physical conditions of the simulated system was the same as for the base-case at 40 C and a CO_2 pressure of 100 bars. At a reactive surface area that is equal to the estimated S_0 all porosity is lost after approximately 1000 years as stilbite and siderite fills the pore space. If the reactive surface area is reduced by one order of magnitude (i.e. the base case) nearly 1/10 of the original 10% porosity is preserved. Further reductions by one and two orders of magnitude lead to smaller changes and at three orders of magnitude reduction relative to S_0 almost no change is observed (Figure 6).

System 2: The potential for carbonate growth in a H_2O-saturated $scCO_2$ phase

The reaction between H_2O dissolved in $scCO_2$ and basalt was simulated at 100 bar pressure and 40 C. The initial amount of water was 0.003 Kg and no H_2O was

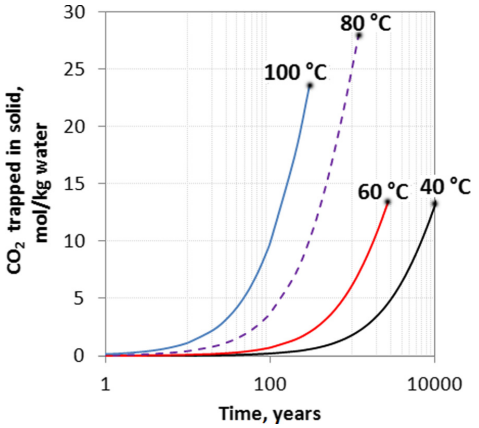

Figure 4 CO_2 trapped in solids for 40 to 100 C simulations at 100 bar CO_2 pressure. A cut-off value is used when all pore space is filled up with the secondary phases (see Figure 5). The simulations suggest that the total amount of secondary carbonates that form is dictated by the available pore space and the thermodynamic stability of secondary phases rather than temperature, whereas carbonate generation rates depend on the exponential increase of basalt dissolution rates with temperature.

allowed to enter the system. This is an ideal end-member case and serves to illustrate the carbonation potential in a volume with limited hydration potential.

As secondary phases such as stilbite formed, water was rapidly consumed and most gone after 45 years

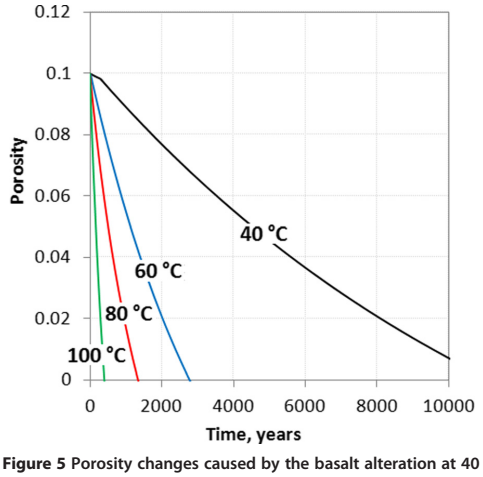

Figure 5 Porosity changes caused by the basalt alteration at 40 to 100 C. Secondary hydrated species and carbonates incorporate the H_2O and CO_2 masses into the solids and clogs the pore space. As reaction rates increase exponentially with temperature, the pore space is filled up faster at the higher temperatures.

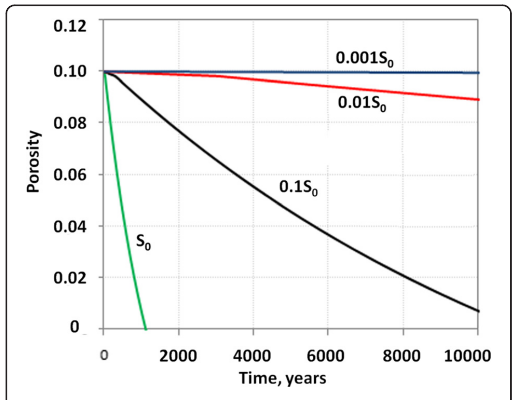

Figure 6 Porosity changes caused by the basalt alteration at 40 C and specific surface areas ranging from S_o (estimated total basalt surface area) down to a three orders of magnitude reduction. The base case specific surface used was S_o/10.

(Figure 7a). At this point stilbite was unstable and supplied water until all water was consumed after approximately 100 years (Figure 7a). Following the basalt hydration, siderite and ankerite formed from the released Ca, Mg, and Fe, with a final total amount of 0.2 moles CO_2 consumed per liter pore space after 100 years (Figure 7b). If H_2O had been allowed to dissolve into the $scCO_2$ phase from residual aqueous phases trapped in the smaller pores, the carbonation potential would have been larger. This process is however, to the knowledge of the authors, not possible to simulate using the PHREEQC code, and was therefore outside the scope of this study.

System 3: 1D diffusion of CO_2 into the CRB aquifer

To see how the basalt reacted under different CO_2 pressures, we defined a 1D diffusion–reaction simulation. This provided us with basalt-CO_2 interactions over a continuous range of CO_2 pressures from the background 1 bar up to the maximum 100 bars. The system corresponds to a stagnant zone presented as a column with one end close to the boundary of the injected CO_2 plume and the other end further away from the plume (Figure 1). The distance reached for the CO_2 into the column is given by the balance between diffusive transport and removal of carbon by secondary carbonate formation. We therefore varied reaction rates from no reaction giving the maximum lengtht of diffusive transport, and up to the base-case rate given by a reaction surface area 1 order of magnitude lower than the estimated physical surface area. Figure 8 shows pH, dissolved CO_2 (mol/Kgw) and amount of secondary carbonate formed in the 1D column. As CO_2 diffuses into the column pH drops to approximately 4 at full

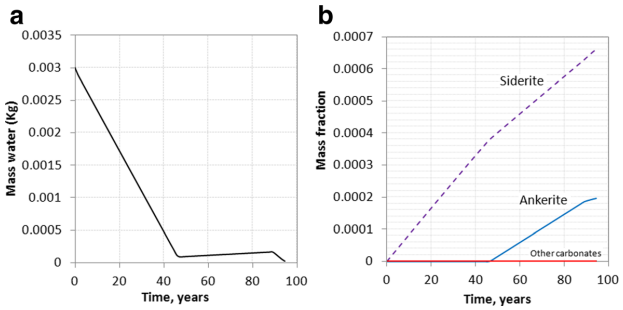

Figure 7 Basalt alteration in the $scCO_2$ rich phase with initial 3 grams of water per liter pore space. A) as zeolites form H_2O is consumed and the water activity is reduced. After approximately 45 years most water is consumed, whereas all is gone before 100 years. **B**) siderite formed the secondary carbonate initially followed by ankerite.

saturation. The depth of diffusion into the 1D column is approximately 40 meters at 1000 years if no carbonate forming reactions occur (Figure 8a). The penetration depth decreased rapidly if reactions were allowed as siderite formed and pulled carbon out of aqueous system (Figure 8b, c). At the highest reaction rate (base-case), CO_2 diffused less than 10 meters into the column as approximately 13 moles/Kgw of siderite formed at the end of the 10000 years simulation (Figure 8d). Siderite formed at greater depth if the reactive surface area was reduced by another order of magnitude, but less formed in total (Figure 8d).

Discussion

Uncertainty on the reactive surface area

The reactive surface area is considered as a major source of uncertainty (e.g., [20,34]) and this leads to corresponding high uncertainties in timing and extent of reactions as dissolution rates have a first order dependence on reactive surface areas. Weathering rates in nature are commonly observed to be 1–3 orders of magnitude lower than in laboratory experiments (e.g., [20,21,34]), and this may in part be explained by differences in reactive and physical (total) surface area between experimental and natural systems. We assumed in this study a base-case reactive surface area 1 order of magnitude lower than the estimated physical surface area for the basalt. A further two orders of magnitude reduction in the reactive surface area, which is within the range of values expected for natural systems, resulted in little basalt alteration and only minor reduction of porosity (see Figure 5). A better understanding of the surface area of porous basalt and the effect of time (aging) on features such as dislocation densities and reactive surface areas are therefore required to understand the potential for CO_2 mineral storage in basaltic rocks.

Uncertainty on the choice of secondary phases used in the model

Growth rate experiments of carbonates such as magnesite and dolomite have shown that the activation energy is high and that growth is negligible at low temperatures (e.g., [35-37]). Dissolution rate studies of siderite suggests that the reaction rate is intermediate between calcite and magnesite [38,39], and growth rate data suggest that siderite may form down to room temperature [40]. Data on ankerite dissolution and growth is to the knowledge of the authors not known. The crystallographic and physical characteristics of ankerite do resemble those of dolomite and siderite, and the chemistry is related to dolomite with the Mg^{2+} substituted by various amounts of Fe^{2+} and Mn^{2+}. If the growth rate is close to the magnesian carbonates such as dolomite and magnesite [41,42], the amount that may form during low-temperature alteration is likely low. In this case, more iron would be available for siderite growth. If on the other hand the growth rate is closer to siderite, we would expect ankerite or other FeMg solid solution carbonates to grow during low-temperature alteration.

One uncertainty related to the local-equilibrium assumption is on the growth retention time for the secondary carbonates. The local-equilibrium assumption predicts growth of the secondary phases as soon as an infinitesimally small supersaturation is reached [23]. The time it takes to nucleate sufficient mass to initiate a significant growth may however be hundreds to thousands of years for some secondary phases [31]. There are no nucleation rate data for siderite and ankerite and the retention time is hence unknown.

Finally, the total potential for secondary carbonate growth may be affected by the amount of magnesium and iron that enters ferromagnesian calcites. As a significant fraction of the metal cations may substitute for calcium (e.g., [43]), a iron-magnesium rich calcite may

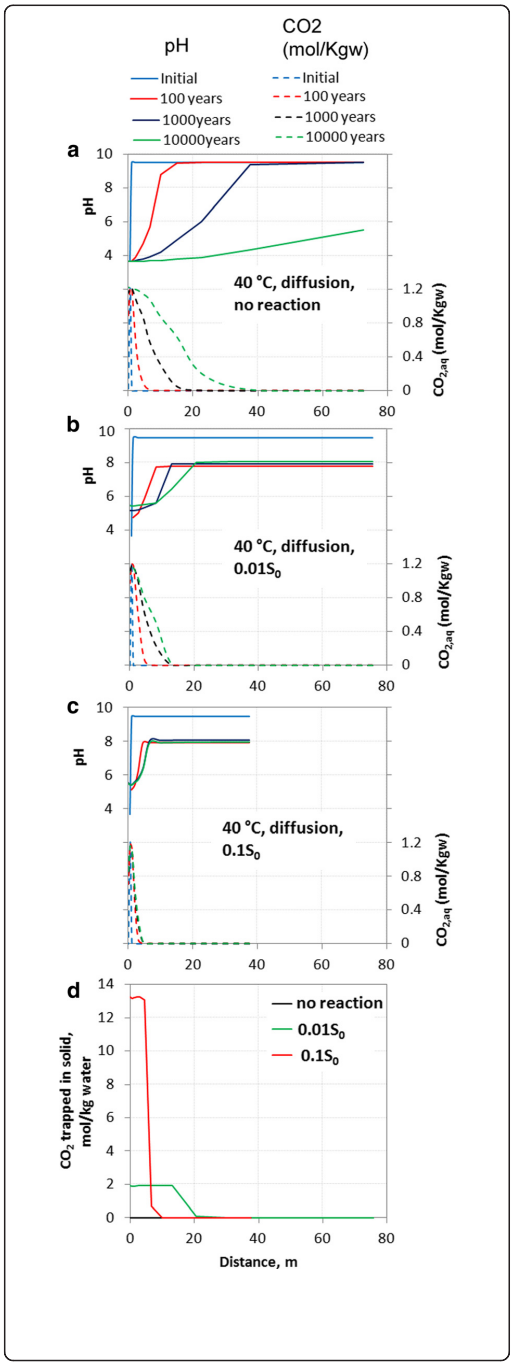

Figure 8 1D reaction–diffusion of CO_2 into permeable basalt. Partial pressure of the inlet boundary was fixed at 100 bar and with a column temperature of 40 C. As consumption of CO_2 by siderite growth affects the depth of CO_2 diffusion, we ran a sensitivity study on reactive surface area going from no reaction **(a)** up to the base case **(c)**. Finally the amount of CO_2 trapped as solid carbonate (siderite) was compared for the base case and reduced reactive surface area **(d)**. We see that the reaction rates strongly constraint the depth of the column affected by the CO_2 diffusion.

potentially form rather than ankerite and thereby reduce the amount of siderite formed.

Comparisons to experiments, numerical simulations and natural analogues of basalt-CO_2 interactions

Our simulations suggest that the potential for carbonate growth is limited to siderite or FeMg carbonates at low temperatures as secondary phases such as zeolites outcompeted the carbonates for calcium. We here compare our simulated results with reported data on CO_2-basalt interactions from laboratory experiments, natural analogues, and other reported numerical simulations.

The reactivity of CRB and other continental flood basalts are available from the long-term (months to years) laboratory experiments done by Schaef and coworkers [6,24]. In these experiments basalt samples from USA, India, South Africa, and Canada were reacted with CO_2 at about 100 bars and 60 to 100 C. Reacted samples from these experiments showed generation of Ca-rich carbonates interpreted as calcites with minor siderite and magnesite. In experiments on CRB using mixtures of H_2S and CO_2 at 60 C and 100 bar and run for 181 days, pyrite (FeS_2) formed together with Mg-Fe poor calcite and a Ca-poor Fe-carbonate [6]. Our simulations at the same temperatures show rapid formation of siderite (60 C) or siderite and magnesite at higher temperatures (Figure 3). Our simulations do not predict any calcite growth as the calcium activity is lowered by zeolite formation. Calcite would however form in our models if the zeolites were not allowed to form at local equilibrium, and possibly if a magnesian ferroan (solid solution) calcite was used in the model instead of the pure end-member calcite. Therefore, the apparent difference between our model and the experiment may be caused by our use of the local equilibrium assumption, whereas the zeolites in the laboratory experiments did not form at low temperatures due to slow kinetics. Recent experiments on basalt dissolution support the preferential release of Mg and Fe over Ca at acidic conditions [22], suggesting that the MgFe-carbonates will dominate as secondary carbonates during CO_2 storage in basalt.

Our numerical simulations share some similarities to other works such as by Marini [18] and Gysi [44], but

our model and hence the outcome is different in several aspects. The most comprehensive work done earlier is the numerical simulations done by Marini [18] on the reactivity of crystalline and glassy CFB following CO_2 storage. The initial mineralogy was similar to our study whereas the temperature of 60 C was slightly higher than our base case 40 C. In [18] the CO_2-basalt interactions were stretched to last for more than 280000 years compared to our 10000 years perspective. The main differences between our model and [18] are on the choice of secondary mineral assemblage, and on the focus of limiting factors such as the availability of water for hydration in the present work. The lack of zeolites and hydrous phases other than kaolinite and goethite in [18] made Ca available for secondary carbonates and the total potential for carbonate formation was higher than in our work. Marini allowed dolomite and magnesite to form at 60 C, whereas our simulations only produced siderite at the similar conditions. Moreover, the formation of dawsonite in [18] is still uncertain and possibly limited at high silica activities and with an assemblage of stable NaAl-silicates defined to form [45]. Based on two different approaches, the reactive surface area for basalt was estimated to quite similar values. We estimated a specific surface area of approximately $1.5x10^{-5}$ m^2/g_{basalt} (= 0.14 m^2/Kg water at 10% porosity) based on the A_p/V_p values estimated by [46] and reported in [5], and reduced this value by one order of magnitude to get the reactive surface area. Marini used a geometric model giving a reactive surface area of 0.41 m^2/Kg water. The higher reactive surface area and higher temperature of [18] resulted in faster reactions and more rapid clogging of the pore space (within a few years). Studies of natural basalt systems at similar or higher temperatures may give some insight into how fast pore space is clogged by basalt hydration or carbonation, and this should be used to improve the estimates of reactive surface areas of basalt for future studies.

Another numerical study on low-temperature (25 C, 30 bar CO_2) basaltic glass alteration was presented by Gysi et al. [44]. Again a main difference is on the choice of secondary minerals. Gysi et al. [44] allowed dolomite, magnesite, and Fe-Mg carbonate to form together with calcite and siderite, whereas we did not allow other Mg-Fe carbonates to form than ankerite. As previously stated, the low-temperature formation of dolomite and magnesite is not likely because of the high apparent activation energy and small kinetic coefficients for the growth of Mg-carbonates [35-37]. Other carbonates such as siderite and potentially FeMg-calcites are more likely to form at these low temperatures. The high reactive surface area used in [44] is based on a geometric model for glass fragments, and is hence not directly comparable with the surface area estimated for a vesicle pore space of a solid basalt. Although no inverse modeling was done to estimate the reactive surface area of the basalt in [44], fragmented basaltic rocks such as hyaloclastite breccias are expected to have significantly higher reactive surface areas than porous solid basalts, and they are therefore correspondingly more reactive.

One example of a natural analogue that shed light on CO_2 basalt interactions is the CO_2 charged basalt hosted groundwaters at Hekla, Iceland. Solution aqueous species sampled from natural cold springs and rivers here showed a drop in total inorganic carbon (TIC) that was interpreted to result from considerable formation of secondary carbonate phases such as calcite [47]. Reaction path modeling of the system suggests however that the carbonate formation is associated with high pH in accordance with the low TIC in the sampled waters. This system is therefore different from basalt CO_2 storage projects where higher CO_2 pressures may be maintained over time and the pH is lower. In addition to calcite, dolomite was also suggested as a potential storage host for the low temperature reactions in Hekla [47]. This may however be questionable as long-term laboratory experiments at room temperature have failed to form dolomite even at significant super saturations [48], explained by the high activation energy for dolomite growth [32,41]. Another natural analogue that more closely corresponds to industrial CO_2 storage is the basalt-hosted petroleum reservoir on Nuussuaq, West Greenland. In this system the bulk carbonate formation appears to have occurred as secondary weathering products. Other alteration products such as zeolites and oxides were replaced by dolomite, magnesite, siderite, and calcite at temperatures of 70–120 C [49]. Therefore, taking into account the basalt weathering products and not only primary basalt minerals appears to be vital in estimating the total potential for secondary carbonate formation and the long-term potential for CO_2 storage in basalt systems.

Summary and conclusions

Simulations of closed-system (P_{CO2} = 100 bar, 40 C) and 1D reaction–diffusion (P_{CO2} = 0–100 bar, 40 C) alteration of basalt suggest that the potential of secondary carbonate formation is limited to siderite at low temperatures as divalent metal cations are preferentially consumed by zeolites and oxides. Higher temperatures 60 – 100 C appear to be in favor of secondary carbonate formation, allowing the precipitation of carbonates such as magnesite, siderite and possibly dolomite and other FeMg carbonates (ankerite). Given an unlimited source of CO_2 (fixed CO_2 pressure), the total amount of CO_2 stored as solid carbonates is orders of magnitude higher than the 1–2 mol/Kg water solubility in the formation water (Figure 4). The total amount trapped might

however be reduced if CO_2, H_2O or pore space are limiting factors. The formation of secondary hydrous and carbonate phases increases the volume of solids and the porosity is correspondingly reduced (Figure 5). This together with the immobilization of CO_2 by solid carbonate formation is in favor of safe long-term storage of CO_2 in basaltic aquifers.

Competing interests

We have no competing interests with any organization to publish the manuscript 'On the potential for CO2 mineral storage in continental flood basalts – PHREEQC batch- and 1D diffusion-reaction simulations'.

Authors' contributions

VTH Pham has made substantial contributions to conception and designs the manuscript. Her contributions are to acquisition of data, analysis and interpretation of data. PA did revising and has given final approval of the version to be published. HH involved in drafting the manuscript, writing methodology part and revising of the final version. All authors read and approved the final manuscript.

Acknowledgements

We highly appreciated constructive comments and suggestions from the reviewers. This work has been funded by SSC-Ramore (Subsurface storage of carbon dioxide - risk assessment, monitoring and remediation) project and (partially) by SUCCESS centre for CO_2 storage under grant 193825/S60 from Research Council of Norway (RCN). SUCCESS is a consortium with partners from industry and science, hosted by Christian Michelsen Research as.

Received: 1 June 2011 Accepted: 14 June 2012
Published: 14 June 2012

References

1. Holloway S: **Underground sequestration of carbon dioxide–a viable greenhouse gas mitigation option.** *Energy* 2004, **30:**2318–2333.
2. Bachu S, Bonijoly D, Bradshaw J, Burruss R, Holloway S, Christensen NP, Mathiassen OM: **CO_2 storage capacity estimation: Methodology and gaps.** *Int J Greenhouse Gas Control* 2007, **1:**430–443.
3. IPCC: **IPCC Special Report on Carbon Dioxide Capture and Storage**. In *In Prepared by Working Group III of the Intergovernmental Panel on Climate Change*. Edited by Metz B, Davidson O, Coninck H, Loos M, Meyer L. Cambridge, United Kingdom and New York, NY, USA: Cambridge University Press; 2005:442 pp.
4. Oelkers EH, Gislason SR, Matter J: **Mineral Carbonation of CO2.** *Elements* 2008, **4:**333–337.
5. McGrail BP, Schaef HT, Ho AM, Chien Y-J, Dooley JJ, Davidson CL: **Potential for carbon dioxide sequestration in flood basalts.** *J Geophysical Res-Solid Earth* 2006, **111:**1–13.
6. Schaef HT, McGrail BP, Owen AT: **Carbonate mineralization of volcanic province basalts.** *Int J Greenhouse Gas Control* 2010, **4:**249–261.
7. Schaef HT, Windish CF, McGrail BP, Martin PF, Rosso KM: **Brucite [$Mg(OH)_2$] carbonation in wet supercritical CO_2: An in situ high pressure x-ray diffration study.** *Geochim Cosmochim Acta* 2011, **75:**7458–7471.
8. White MD, McGrail BP, Schaef HT, Hu JZ, Hoyt DW, Felmy AR, Rosso KM, Wurstner SK: **Multiphase sequestration geochemistry: Model for mineral carbonation.** *Energy Procedia* 2011, **4:**5009–5016.
9. Parkhurst DL, Appelo CAJ: *User's guide to PHREEQC (version 2) - a computer program for speciation, reaction-path, 1D-transport, and inverse geochemical calculations.*: U.S. Geological Survey, Water-Resources Investigation Report; 1999:312.
10. Soave G: **Equilibrium constants from a modified Redlich-Kwrong equation of state.** *Chem Eng Sci* 1972, **27:**1197–1203.
11. Hellevang H, Kvamme B: **ACCRETE - Geochemistry solver for CO_2-water-rock interactions.** *Proceedings GHGT 8 conference* 2006, **:**8p.
12. Bachu S, Stewart S: **Geological sequestration of anthropogenic carbon dioxide in the western Canada sedimentary basin: Suitability analysis.** *J Can Pet Technol* 2002, **41:**32–40.
13. Coan CR, King AD: **Solubility of Water in Compressed Carbon Dioxide, Nitrous Oxide, and Ethane - Evidence for Hydration of Carbon Dioxide and Nitrous Oxide in Gas Phase.** *J Am Chem Soc* 1971, **93:**1857–1862.
14. Sabirzyanov AN, Ilin AP, Akhunov AR, Gumerov FM: **Solubility of water in Supercritical carbon dioxide.** *High Temp* 2002, **40:**203–206.
15. Bahar M, Lui K: *Measurement of the diffusion coefficient of CO_2 in formation water under reservoir conditions: Implication for CO_2 storage, Society of Petroleum Engineers, SPE Asia Pacific Oil and Gas Conference and Exhibition, 20–22 October 2008*. Perth, Australia;; 2008.
16. Palandri JL, Kharaka YK: *A Compliilation of Rate Parameters of Water-Mineral Interaction Kinetics for Applicatin to Geochemical Modeling. U.S. Geological survey, Open report.:* ; 2004:1068.
17. Gislason SR, Oelkers EH: **Mechanism, rates, and consequences of basaltic glass dissolution: II. An experimental study of the dissolution rates of basaltic glass as a function of pH and temperature.** *Geochim Cosmochim Acta* 2003, **67:**3817–3832.
18. Marini L: *Chapter 7: Reaction path Modelling of geological CO_2 sequatration*, In *Geological Sequestration of Carbon Dioxide Thermodynamics, Kinetics, and Reaction Path Modeling.*: Dev Geochem; 2006:319–394.
19. Wolff-Boenisch D, Gislason SR, Oelkers EH: **The effect of fluoride on the dissolution rates of natural glasses at pH 4 and 25 degrees C.** *Geochim Cosmochim Acta* 2004, **68:**4571–4582.
20. White AF, Peterson ML: **Role of reactive-surface-area characterization in geochemical kinetic models**. In *In. Chemical Modeling of Aqueous Systems II.* Edited by Melchior D, *et al.* Washington, DC: ACS Symposium Series, ACS; 1990.
21. White AF, Brantley SL: **The effect of time on the weathering of silicate minerals: why do weathering rates differ in the laboratory and field?** *Chem Geol* 2003, **202:**479–506.
22. Gudbrandsson S, Wolff-Boenisch D, Gislason SR, Oelkers EH: **An experimental study of crystalline basalt dissolution from $2 \leq pH \leq 11$ and temperatures from 5 to 75 C.** *Geochim Cosmochim Acta* 2011, **75:**5496–5509.
23. Helgeson HC: **Evaluation of Irreversible Reactions in Geochemical Processes Involving Minerals and Aqueous Solutions .I. Thermodynamic Relations.** *Geochim Cosmochim Acta* 1968, **32:**853–877.
24. Schaef HT, McGrail BP, Owen AT: **Basalt-CO_2-H_2O Interactions and Variability in Carbonate Mineralization Rates.** *Energy Procedia* 2009, **1:**4899–4906.
25. Schaef HT, McGrail BP: **Dissolution of Columbia River Basalt under mildly acidic conditions as a function of temperature: Experimental results relevant to the geological sequestration of carbon dioxide.** *Appl Geochem* 2009, **24:**980–987.
26. Blake S, Self S, Sharma K, Sephton S: **Sulfur release from the Columbia River Basalts and other flood lava eruptions constrained by a model of sulfide saturation.** *Earth Planet Sci Lett* 2010, **299:**328–338.
27. Neuhoff PS, Fridriksson T, Arnorsson S, Bird DK: **Porosity evolution and mineral paragenesis during low-grade metamorphism of basaltic lavas at Teigarhorn, eastern Iceland.** *Am J Sci* 1999, **299:**467–501.
28. Neuhoff PS, Rogers KL, Stannius LS, Bird DK, Pedersen AK: **Regional very low-grade metamorphism of basaltic lavas, Disko-Nuussuaq region, West Greenland.** *Lithos* 2006, **92:**33–54.
29. Stefansson A, Gislason SR, Arnorsson S: **Dissolution of primary minerals in natural waters - II.** *Mineral saturation state. Chem Geol* 2001, **172:**251–276.
30. Reidel SP, Johnson VG, Spane FA: *Natural gas storage in basalt aquifers of the Colombia Basin, Pacific Northwest USA: A guide to site characterization*. H: Report Pacific Northwest National Laboratory; PNNL-13962; 2002.
31. Pham VTH, Lu P, Aagaard P, Zhu C, Hellevang H: **On the potential of CO_2-water-rock interactions for CO_2 storage using a modified kinetic model.** *International Journal of Greenhouse Gas Control* 2011, **5:**1002–1015.
32. Reidel SP: **A lava flow without a source: the cohassett flow and its compositional components, Sentinel Bluffs Member, Columbia River Basalt Group.** *J Geol* 2005, **113:**1–21.
33. Peuble S, Godard M, Gouze P, Luquot L: **CO_2 sequestration in olivine rich basaltic aquifers: a reactive percolation experimental study.** *Geochim Cosmochim Acta* 2009, **73:**A1635.
34. Velbel MA: **Constancy of silicate-mineral weathering-rate ratios between natural and experimental weathering: implications for hydrologic control of differences in absolute rates.** *Chem Geol* 1993, **105:**89–99.
35. Saldi GD, Jordan G, Schott J, Oelkers EH: **Magnesite growth rates as a function of temperature and saturation state.** *Geochim Cosmochim Acta* 2009, **73:**5646–5657.
36. Arvidson RS, Mackenzie FT: **The dolomite problem; control of precipitation kinetics by temperature and saturation state.** *Am J Sci* 1999, **299:**257–288.

37. Arvidson RS, Mackenzie FT: **Tentative kinetic model for dolomite precipitation rate and its application to dolomite distribution.** *Aquat Geochem* 1996, **2:**273–298.
38. Golubev SV, Bébnézeth P, Schott J, Dandurand JL, Castillo A: **Siderite dissolution kinetics in acidic aqueous solutions from 25 to 100 C and 0 to 50 atm pCO_2.** *Chem Geol* 2009, **265:**13–19.
39. Pokrovsky OS, Golubev SV, Schott J, Castillo A: **Calcite, dolomite and magnesite dissolution kinetics in aqueous solutions at acid to circumneutral pH, 25 to 150 C and 1 to 55 atm pCO_2: New constraints on CO_2 sequestration in sedimentary basins.** *Chem Geol* 2009, **265:**20–32.
40. Greenberg J, Tomson M: **Precipitation and dissolution kinetics and equilibria of aqueous ferrous carbonate vs temperature.** *Appl Geochem* 1992, **7:**185–190.
41. Arvidson RS, Mackenzie FT: **Tentative Kinetic Model for Dolomite Precipitation Rate and Its Application to Dolomite Distribution.** *Aquat Geochem* 1997, **2:**273–298.
42. Saldi GD, Jordan G, Schott J, Oelkers EH: **Magnesite growth rates as function of temperature and saturation state: An HAFM study.** *Geochim Cosmochim Acta* 2009, **73:**A1149.
43. Busenberg E, Plummer LN: **Thermodynamics of magnesian calcite solid-solutions at 25 C and 1 atm total pressure.** *Geochim Cosmochim Acta* 1989, **53:**1189–1208.
44. Gysi AP, Stefansson A: **Numerical modelling of CO_2-water-basalt interaction.** *Mineral Mag* 2008, **72:**55–59.
45. Hellevang H, Declercq J, Aagaard P: **Why is dawsonite absent in CO_2 charged reservoirs? *Oil & Gas Science and Technology - Re.*** *IFP Energies nouvelles* 2011, **66:**119–135.
46. Saar MO, Manga M: *The relationship between permeability, porosity, and microstructure in vesicular basalts.*: Master Thesis, Univ. of Oregon, Eugene; 1998:91.
47. Flaathen TK, Gislason SR, Oelkers EH, Sveinbjornsdottir AE: **Chemical evolution of the Mt. Hekla, Iceland, groundwaters: a natural analogue for CO_2 sequestration in basaltic rocks.** *Appl Geochem* 2009, **24:**463–474.
48. Land LS: **Failure to precipitate dolomite at 25 degrees C from dilute solution despite 1000-fold oversaturation after 32 years.** *Aquat Geochem* 1998, **4:**361–368.
49. Rogers KL, Neuhoff PS, Pedersen AK, Bird DK: ***CO_2 metasomatism in a basalt-hosted petroleum reservoir, Nuussuaq, West Greenland.*** *Lithos* 2006, **92:**55–82.

doi:10.1186/1467-4866-13-5
Cite this article as: Van Pham *et al.*: On the potential for CO_2 mineral storage in continental flood basalts – PHREEQC batch- and 1D diffusion–reaction simulations. *Geochemical Transactions* 2012 **13**:5.

Paper 3

Assessment of CO_2 injection into the south Utsira-Skade aquifer, the North Sea, Norway

By:

V.T.H. Pham, I.T. Gjeldvik, F. Riis, E. K. Halland, P. Aagaard.

International Journal of Energy

(Reviewed in Jan. 2013)

Paper 4

Kinetic modeling of CO2-water-rock interactions

By:

H. Hellevang, V.T.H. Pham, P. Aagaard.

International Journal of Greenhouse Gas Control

(Accepted for publication 2013)

Extended Abstract

Numerical modeling including hysteresis properties for CO_2 storage in Tubåen Formation, Snøhvit field, Barents Sea

By:

V.T.H. Pham, T. E. Maast, H. Hellevang, P. Aagaard.

Energy Procedia 2011, 4: 3746 – 3753